THE UNIVERSITY OF OKLAHOMA HEALTH SCIENCES CENTER

GRADUATE COLLEGE

Aerosol Capture Efficiency of a Prototype Dental Aerosol Shield

A THESIS

SUBMITTED TO THE GRADUATE FACULTY

in partial fulfillment of the requirements for the degree of

Master of Science degree

BY

ENEOJO ONUCHE

Oklahoma City, Oklahoma

2021

Aerosol Capture Efficiency of a Prototype Dental Aerosol Shield APPROVED BY:

_____

Evan Floyd, Ph.D., Assistant Professor
Department of Occupational and Environmental Health Sciences

_____

Changjie Cai, Ph.D., Assistant Professor
Department of Occupational and Environmental Health Sciences

_____

K.A.N Aithinne, Ph.D., Assistant Professor
Department of Occupational and Environmental Health Sciences

THESIS COMMITTE

COPYRIGHT

BY

ENEOJO ONUCHE

DECEMBER 17, 2021

ACKNOWLEDGEMENTS

I would like to appreciate the almighty God for all His blessings and grace that I enjoyed all through this program. I am sincerely thankful for all the support, dedication, and commitment I received from my committee on this project, as without them, none of this would be possible. A special thank you to my academic advisor and mentor, Dr. Evan Floyd, for his outstanding support and guidance throughout my time in the program. I would like to thank Dr. Changi Cai for committing so much of his time in developing the Python Code that was used for statistical analyses of the data. Thank you to Dr. K.A.N Aithinne for her encouragement and help. Special thanks to my committee members from the College of Dentistry, Dr. Fernando Esteban Florez and Ms. Kim Graziano for their wonderful collaboration and support as well as providing us with the opportunity to assess the aerosol capture efficiency of their prototype named Pro-Tect-Shield (PTS).

I would also like to acknowledge the National Institute of Occupational Safety and Health (NIOSH) training grant which provided me with stipends and paid for my tuitions from August 2019 to June 2021. I would also like to thank the Hudson College of Public Health for awarding me with the Ronald L. Coleman and the Board of Certified Safety Professionals OEH scholarships, which provided financial support during my time at the University of Oklahoma Health Sciences Center. The constant support of my wife, Sinmi and my daughter, Anora, was invaluable to my studies. I appreciate all the support and encouragement from my friends, Stephen Bonanni, Toluwanimi Oni and John Skender. Thanks to all the graduate faculty of the Hudson College of Public Health for their commitment and dedication to teaching and helping their students. Also, thank you to the staff of the Graduate College and the Hudson College of Public Health, Office of Student Services, and Office of Finance and Administration for their support.

Lastly, I would like to deeply appreciate my professors at the Department of Occupational and Environmental Health professors: Dr. Margaret Phillips, Dr. Evan Floyd, Dr. Changjie Cai, Dr. Jooyeon

Hwang, Dr. K.A.N Aithinne, Dr. Gregory Day and Professor Tommy Klepper, Jr., Esq., M.P.H. Your diligence and commitment to students' success have inspired my inner confidence to keep pursuing my career goals.

ABSTRACT

Aerosols and splatter generated during dental procedures have the potential to transmit infectious diseases to patients and dental personnel. This study evaluated the performance of the newly developed aerosol evacuation device named as Pro-TecT-Shield (PTS). The objective of this study was to evaluate PTS aerosol capture efficiency at distinct flow rates for various particle sizes, and the impact of aerosol plume velocity on PTS performance as well as the effects of PTS placement relative to aerosol plume.

This study was performed in 2 phases. Phase 1 involved suction airflow determination for high-volume extractors (HVE) installed at the Miranda Clinic of the University of Oklahoma Health Sciences Center College of Dentistry (OUCOD) and plume velocities that are typically generated during the delivery of routine dental care. This phase revealed that HVE flowrates ranged from approximately 104 to 194 liters per minute (Lpm), and plume velocities varied from approximately 3 to 62 feet per minute (Ft/min) as measured while simulating dental procedures (cavity preparation or dental plaque removal using a high-speed turbine and an ultrasound, respectively; note that air/water spray was used in both simulations). In Phase 2, PTS capture efficiency was determined resolved by the diameter of particles (diameters from 0.3 μm to 5 μm). Other influencing factors such as HVE flowrates (100 and 200 Lpm), aerosol plume velocities (6, 25, 50 and 100 Ft/min) and PTS spatial positioning were also investigated as they are known to influence the efficacy of aerosol mitigation devices, such as the PTS. A NaCl solution (at 2%) was used together with a Collison Nebulizer (3 Jet, CH Technologies, Westwood NJ, USA) to generate the test aerosols. A laser aerosol spectrometer (TechnIK GmbH & Co. KG, Model 1.108) was used to determine PTS capture efficacy for particles with varied diameters (< 0.3 μm up to 20 μm). Data reduction and analysis was performed in Jupyter Notebook Software (version 6.3.0) with a Python code developed by Dr. Changjie Cai using mixed effect regression model.

Findings from this study have demonstrated that the PTS was significantly ($p = 0.003$) more effective exhausting particles of small diameters (0.3 μm – 5 μm) when operated at 200 Lpm flowrate as compared to 100 Lpm. Collection efficiency was observed to vary as a function of plume location on the PTS.

At both HVE flowrates, overall collection efficiency decreased with the increase in distance from the vacuum manifold. At HVE flowrate of 200 Lpm, and all plume velocities (6, 25, 50 and 100 Ft/min), average collection efficiency ranged from 70% - 100% at plume locations closest to PTS suction manifold. As such, the PTS should be positioned to intercept the aerosol plume as close to the suction manifold as practicable during the delivery of routine dental care. The use of PTS in this manner will minimize the risk of infectious disease transmission in dental settings.

TABLE OF CONTENTS

LIST OF TABLES

TABLE

LIST OF FIGURES

CHAPTER 1

BACKGROUND AND LITERATURE

An aerosol can be simply defined as tiny particles or droplets suspended in the air which can be either liquid or solid particles (Hinds, 1999). Particle size-selective sampling refers to the collection of particles of varying sizes that has the potential to penetrate and affect deeper regions of the respiratory system (Brown, Gordon, price, and Asgharian, 2013). In an occupational context, aerosols fall into three broad size categories, inhalable, thoracic and respirable fractions. These are defined as the fraction of particles in air that can be (i) aspirated through the nose or mouth during normal breathing, (ii) can travel to the larynx and upper airways following inhalation, (iii) can be inhaled and travel beyond the larynx and ciliated airways, respectively (Brown et al., 2013).

A Systematic review of the literature was conducted using Ovid, PubMed, and Science Direct databases. Secondary sources included Google Scholar, American Dental Association (ADA), Centers for Disease Control and Prevention (CDC), Semantic Scholar and the Journal of Multidisciplinary Care. A study was included for final extraction when it met one or more of the following inclusion criteria: aerosols, dental aerosols, bioaerosols, infection control, aerosol particle, particle size, composition, dentistry, and healthcare aerosols. Studies published in languages other than English were excluded from the literature review.

It has been shown that particle sizes influence the site of deposition within the respiratory tract and the survival of microorganisms in aerosols. Small particles with sizes that are similar to that of a bacterium (1 to 5 μm) are typically deposited in the alveoli, while particles with dimensions that greater than 10 μm, tend to deposit in the upper respiratory tract (Thomas, et al., 2008). Bioaerosols contain particles of biological origin that have been suspended in air. Aerosols and splatter generated during dental procedures may come from variety of sources such as dental instrumentation, saliva, blood, and respiratory sources, (Geisinger, 2020). During dental treatments, aerosols are emitted from near patients' mouths into the surrounding air, with a fraction remaining airborne for extended periods of time, thus creating the potential for

the transmission of respiratory infectious diseases to the dentist, dental personnel, support staff and patients. Qualitative and quantitative analysis of the composition of dental aerosols is extremely difficult as they vary with each patient, operative site, and type of procedure (Harrel and Molinari, 2004).

Dental procedures that generate aerosols consist of drilling, cutting, filling, polishing, and cleaning. Specifically, dental handpieces such as high-speed air-turbines and ultrasonic scalers are known to generate visible aerosol plumes and conspicuous splatter. A cloud of particulate matter (PM) is often clearly visible to the naked eye during dental procedures with ultrasonic scaling. PM_{10} are inhalable particles with diameters that are less than or equal to (≤) 10 μm while $PM_{2.5}$ are fine inhalable particles that are generally ≤ 2.5 μm in diameter (Environmental Protection Agency, 2021). Splatter is a term ascribed to aerosols with particles larger than 50 μm in diameter, they are visible to the naked eye, and not easily inhaled (Micik, 1969). Splatter settles quickly due to the large particle diameter and flies in ballistic trajectories that settle on nearby surfaces such as equipment, clothes, hair, skin, eyes, and mucous membranes (Gowtham & Deepthi, 2014), while smaller particles tend to be suspended in the air for a longer duration after dental procedures are completed. In addition to inhaling aerosols, other potential routes of disease transmission during dental procedures are by contacts with body fluids, airborne particles from infected patients and contact with contaminated surfaces or instruments (Harrel & Molinari, 2004).

Several studies have reported ultrasonic scalers as the most aerosol and splatter generating devices during dental procedures (Veena, et al., 2020; Harrel and Barnes, 1998; Harrel, 1995; Szymańska, 2007;). Aerosols found within dental clinics could potentially carry infection (Taira, Sasaki, Kimura and Araki, 2009). As a result of the high concentrations of aerosol particles generated by ultrasonic scalers, the ADA and the CDC recommended the use High-Volume Evacuator (HVE) for reducing aerosols and the potential for microbial contamination from dental procedures (Harrel and Barnes, 1998). An HVE is a suction device that draws a large volume of air over a period of time. Results from studies using ultrasonic scalers without the utilization of any type of aerosol reduction device yielded significantly greater quantity of mean colony-forming units (CFUs) at least 6 inches from the patient's mouth (King, et al., 1997; Nulty, 2020).

Computational Fluid Dynamics Simulations of Aerosol Capture Efficiency.

Computational fluid dynamics (CFD) is a modelling process used for studying aerosol particles movement and deposition. It involves the simulation of flow field, particle tracking and post-processing to evaluation the particle deposition information. CFD experimental design involves an aerosol with known particle size distribution and concentration flowing through a controlled volume (Tang and Guo, 2011). Koullapis, Kassinos, and Lin (2015) while investigating the deposition of particles in the lungs using CFD simulations have found that particles with sizes of 10 μm of higher were completely deposited in the mouth-throat region independently of the flowrate investigated. The aerosol concentration at the opening of the control volume is measured to allow the estimation of the fraction of particles that were deposited (Tang and Guo, 2011). According to the results reported, the effects of flowrate on particle deposition, were more evident for particles with diameters between 2.5 and 5 μm. Another finding reported that particles of smaller diameters (0.1, 0.5 and 1 μm) displayed similar deposition behaviors independently of the flowrate investigated. While the findings from Koullapis et al. (2015), focused on particle deposition in respiratory airways, one of the objectives of the present study was to characterize the evacuation efficacy (in function of flowrate and plume velocity) of a novel aerosol containment device (Pro-TecT-Shield, PTS) that was collaboratively developed by the University of Oklahoma Health Sciences Center College of Dentistry (OUCOD) and the Tom Love Innovation Hub at the University of Oklahoma as a response to overcome the occupational challenges imposed by the coronavirus-2019 (COVID-19) pandemic. Devices like the one proposed by researchers at OUCOD are still in the prototyping phase and, therefore, have not yet been subjected to rigorous characterization for capture efficiency.

The present study represents the first opportunity where a highly-controlled and laboratory-based simulation was performed to characterize the performance of the newly-developed PTS. Even though the design of the PTS is simple, it is considered innovative because it allows for a non-turbulent evacuation of air, promotes similar air flowrates across the vacuum manifold, has a transparent splatter shield and is coupled to a structural hose that allows the dentist and the operator to work in an unrestricted manner. The

purpose of the PTS is to efficiently evacuate aerosols while concurrently protecting the operator and assistant from splatter. The device as designed holds the promise to reduce the spread of aerosols with dimensions that not only allow them to remain airborne for long periods of time (up to 41 hours) but, more importantly, may reduce the risk for the transmission of infectious respiratory diseases in dental settings, such as tuberculosis, influenza and COVID-19. A recent study from our group (Esteban Florez et al., 2021) investigated the size-resolved spatial distribution of aerosols in dental settings and the efficacy of PTS to evacuate airborne particles of varying diameters (0.3μm – 20μm) that were nebulized using a 2% sodium chloride solution and a collison nebulizer (20 psi). Results reported have indicated that particles with sizes that are similar to those found in hospitals to have the highest concentration of severe acute respiratory syndrome-coronavirus 2, SARS-CoV-2 (0.25 μm – 0.50 μm) are capable to efficiently spread throughout the area of a large operatory room at the OUCOD, and that the PTS significantly decreased particles' concentrations detected up to 8-56-fold. The PTS was demonstrated to have higher efficacy for particles with dimensions between 0.25 μm – 0.50 μm.

Shahdad et al. (2020), investigated the efficacy of an extraoral scavenging device (EOS) on splatter contamination in dental setting with either closed or open dental operatories. The EOS was vertically positioned at 15-20 cm from the oral cavity and horizontally in a 5 o'clock position. The device was operated at 310 cubic feet per hour (Ft^3/hr) and air/water coolant sprays were adjusted to flow rates of 29.3, 36.8 and 140.6 mL/minute for air-turbine, ultrasonic scaler and triple syringe, respectively. The utilization of the EOS was demonstrated to not only significantly decrease contaminations levels observed in operatory sites by 75%, but also to mitigate the incidence of contamination by 20%. The system proposed was shown to also decrease the mean levels of contamination on personal protective clothing by 33% and 76% in open and closed operatories, respectively. Even though significant levels of contamination were visually detected at distances around 1.34 m from the emission source in both types of operatories, the study was not capable of visually detecting contaminations caused by aerosols containing small particles at distances beyond 1.34 m due restrictions in visual acuity.

Since the operator and dental assistant assume different positions during the delivery of routine dental care (e.g., cavity preparation, scaling and root planning), the distribution of droplets and splatter reported may have been affected by the fixed position of the EOS, which not only limits the efficacy of the device proposed, but also restricts the ability of dental professionals to deliver care. Since large particles display ballistic trajectories, and taking into consideration that the point of aerosol emission changes according to the type of dental care being delivered and the location within the oral cavity, then it becomes obvious, that the efficacy of any aerosol evacuation system will be impacted by its spatial position (x, y and z) relative to the source that generates the aerosol. The newly-developed PTS can be easily adjusted (vertical, horizontal, and diagonal) by the assistant or the operator to best fit the aerosol control needs during the delivery of dental care, and because of that feature, the PTS was demonstrated to efficiently intercept and exhaust larger particles.

Devices that isolate the field of operation (e.g., rubber dams and Isolite systems) and saliva ejectors are commonly used during the delivery of different dental treatments. Each of these devices have been studied for effectiveness in reducing aerosols produced by ultrasonic scalers (Avasth, 2018). In dentistry, high-volume evacuation systems (HVE) are suction devices with large openings (diameters ≥ 8.0 mm) that are typically connected to the vacuum lines of dental chairs and are capable of evacuating large volumes of air between 100 - 200 Lpm). During AGDP, the assistant typically handles the HVE to guide and aim the device in a manner to increase the system's efficiency and to visually reduce the sprays generated during dental procedures (Harrel and Molinari, 2014).

Figure 1. Dental mirror coupled with a high-volume evacuation system. The intra-oral positioning of the HVE and its close proximity to the source (ultrasonic scaler) allows for the efficient removal of aerosols during AGDP (Avasth, 2018).

HVE was reported to be an effective solution for reducing dental aerosol concentrations as well as minimizing the risk of contamination in dental clinics (Harrel, 1996; Jacks,

2002; Klyn, 2001; Jacks, 2002). No studies have reported absolute effectiveness of HVE in eliminating the risk of spreading of airborne infectious respiratory diseases in dental settings. As such, it must be emphasized that no single approach can completely eliminate the risk of infection to dental professional and patients. Findings from the present study have shown PTS as an additional layer of infection control that is capable to minimize the exposure risks to contaminated aerosols and splatter.

In addition of using HVE for reducing aerosols and microbial contamination in dental settings, the utilization of 2% chlorhexidine as coolant for ultrasonic scalers was demonstrated effective at reducing microbial contamination when compared to coolants with other sanitizing agents such as povidone iodine or simple distilled water (Jawade, et al., 2016). It is possible to reduce the risk for the spreading of airborne infectious respiratory diseases in dental settings by using a high-volume evacuation system that intercepts exhaled air, aerosols, water, and saliva droplets that are generated either by patients or instruments during routine dental care.

Within the dental community aerosols are commonly differentiated based on particle size. Aerosol particles greater than 50 μm are considered splatter, while particles less than 50 μm are considered "aerosol". In addition, 90% of aerosol particles generated during dental procedures are less than 5 μm in diameter. Furthermore, droplet nuclei are particles less than 10 μm, because particles smaller than 10 μm can fully evaporate before reaching the floor or nearby surface. Baumann et al. (2018).

Understanding particle size informs the distance the particles are capable of traveling. This is based off the settling velocity and stopping distances of the particles. Aerosol particles can remain airborne for a long time and are easily transported on air currents throughout a dental clinic. It is crucial to understand particle size and particle capture efficiency of a dental aerosol extractor to properly control dental aerosols and protect dental personnel and patients (Milejczak, 2005).

Morawska reported in 2006 that particles with dimensions of 1,000 μm, 100 μm, 10 μm and 1 μm tend to fall by one meter after 0.3, 3, 300 and 30,000 seconds, respectively. According to the authors, this behavior occurs due to drag forces acting on the falling particle that counteract the force of gravity. In short, the larger the particle size the faster it falls, and the smaller the particle size the slower it falls. As

such, exposure of dental professionals and patients to dental aerosols will depend not only on particle size, but also their aerodynamic behavior. Therefore, special attention should be paid to the control of smaller particles because they are capable of remaining airborne for extended periods of times, can travel large distances based on airflow patterns and microorganisms within particles may remain infectious, which in combination, may increase the chances for cross-contamination between patients.

The current concern regarding the potential transmission of infectious respiratory diseases in dental settings precipitates from the fact that aerosol particles with an aerodynamic diameter between 0.5 μm to 10 μm in diameter are typically generated during the delivery of routine dental care and these particles have the potential to penetrate and lodge in the respiratory system, and are known for their ability to spread infectious diseases (Harrel & Molinari, 2004). To further compound the possibility of aerosol transport, water-based particles (droplets) less than 50 μm emitted from a patient's mouth, evaporate quickly after emission which reduces their size and increase their ability to follow air currents. If a droplet is able to evaporate to dryness, it becomes a droplet nuclei which is likely to be very small (1 – 5 μm) with potential to remain airborne for an extended period and follow airflow patterns (Chao et al., 2009). According to the study conducted by Chen et al. (2010), the chances for particles with diameters of 20 μm entering the dental healthcare worker's breathing zone, or removal by the air cleaner is relatively low. This is because they are more likely to be trapped by the body surface or face of patients (Chen et al., 2010).

In a comprehensive study of aerosols and bioaerosol measurements from dental procedures, Polednik (2014) reported the highest increase of submicrometer particle ($PM_{0.02\text{-}1}$ and PM_1) concentrations are during dental grinding and drilling of composite fillings (i.e., 16.1 and 3.4 times higher than the back-ground). The results from this study are similar to those reported by Sotiriou et al. (2008) as it showed a significant variation in aerosol particle concentrations in comparison to background particle levels based on dental procedures. Sotiriou et al. (2008) reported that particles with toxic potential (i.e., aluminum, zinc, silicon, and zirconium) and diameters less than 2.5 μm were typically associated with certain dental bio-materials (i.e., composites, amalgam, etc.) and rotary instruments typically used during cavity preparation and restorative procedures (i.e., finishing and polishing).

According to a recent simulation study that assessed the efficacy of a prototype vacuum helmet (Jia et al., 2021), 100% of airborne droplets and 99.6% of all cough droplets were retained by the vacuum helmet proposed. The vacuum helmet fully encloses the head with an access port at the front to allow for medical procedures and a vacuum port at the top. The system was designed to generate a reversal flow at the access port opening to carry away droplets to the vacuum port before reaching the environment. Two flow rates of 150 ft^3/min and 250 ft^3/min were investigated. While this helmet was quite effective, there are numerous drawbacks that should be noted. The flow rates used are ~25x higher than most HVE systems are capable of supporting. Patients may experience discomfort and claustrophobia while wearing the helmet at such high flow rates. Access to the patient's mouth is restricted due to the rigid front port and this may limit certain tool positions for the dental providers. The reversal flow design will cause contaminated air to be sucked towards the patient and past their face and hair. This undoubtedly will contaminate patients with dental aerosols which is undesirable in many regards. In comparison, the newly-developed PTS will intercept and exhaust dental aerosols generated thereby decreasing the concentrations of contaminated particulates and increasing safety levels for faculty, staff, students and patients. As proposed, the PTS seems to be a cost-effective and highly efficient type of intervention that can be easily implemented without restricting patients' movements or access to patients' mouths, which in turn results in higher acceptability of the technology investigated.

Figure 2: PTS in use at OUCOD. Source: Inside OU News Articles

The oral cavity harbors about 1,000 different microorganisms including bacteria, fungi and viruses. Dental procedures aerosolize saliva, blood dental plaque and oral microorganisms and may promote the airborne transmission of oral organisms with pathogenic potential (Taira et al., 2009). The sizes of aerosol particles generated during dental procedures are similar to the typical sizes of viruses (0.02 μm to 0.2 μm), bacteria (0.2 μm to 2 μm), and fungi (2 μm to 10 μm). Harrel

and Molinari (2004) reported *Mycobacterium tuberculosis* as one of the most serious potential threats in dental aerosols. Based on these findings, it can be inferred that aerosolized saliva and other oral fluids are likely to contain pathogenic organisms responsible for the spreading of infectious respiratory diseases such as tuberculosis, severe acute respiratory syndrome (SARS), common cold, and COVID-19.

Microbial Contamination in Dental Unit Waterlines and Oral Cavities

Dental unit waterlines (DUWL) are plastic tubing designed to transport water from an external reservoir to handheld devices including high- and low-speed rotary instruments, air/water syringes and ultrasonic scalers. These instruments are considered the major source of the aerosols generated during the delivery of dental care (Dutil et al., 2009). As reported in the dental literature, samples of water collected from DUWL contained high numbers of individual bacteria and bacterial aggregates whereas the concentration of bacteria detected in sinks adjacent to operatories were statistically negligible (Putnins et al., 2001).

Chi-Yu et al. (2014) found bacterial aerosol contamination at 100 centimeters (cm) horizontally and 50 cm vertically from a patient's mouth during a dental procedure. In another report, the concentrations of bacteria found in samples collected around the chest of a patient during a dental procedure correlated significantly with the bacteria found in the water samples collected from the DUWL (Zemouri et al., 2020). Based on these findings, it cannot be concluded that surface contamination during dental procedures is caused only by DUWL, as oral fluids are known to contain high numbers of bacteria. As a result, it can be assumed that dental professionals are at high risk for infection by contaminated aerosols due to the nature of dental care and occupational hazards that precipitate from contaminated DUWL and the treatment of asymptomatic patients.

Dental Unit Water Lines Contamination Control

DUWL contamination can be controlled when dental personnel adhere to recommended maintenance protocols for the waterlines. Sodium hypochlorite disinfection regimen, daily draining and purging, and point-of-use filters proved to eliminate microbial contamination in DUWLs (Murdoch-Kinch et al., 1997). Blake (1963) reported that the addition of chlorhexidine to the water in the dental spray reservoir kept it free from bacteria during prolonged use. The study also showed that 0.01 % chlorhexidine solution

kills *Ps. pyocyanea* or *Streptococcus faecalis* within 30 seconds at 55°C and in 40-50 minutes at 20°C, whereas thymol mouthwash solution commonly used by dentists takes 1-2 hours. There are several disinfectants that can be used to decontaminate DUWLs to keep the bacterial load within a safe level. The American Dental Association (ADA) recommended level for bacterial loads in DUWL is less than or equal to 200 CFU/mL. Some of the disinfectants used in DUWLs include Sterilex Ultra and Sanosil (hydrogen peroxide and silver ion based). Using either of these two disinfectants once a week for 15 hours overnight disinfection has proved to keep bacteria concentration in DUWL consistently within the American Dental Association recommendation level. However, bacterial load tends to increase significantly once disinfection is discontinued (Tuttlebee et al., 2002). While dental personnel are encouraged to decontaminate DUWLs using disinfectants, following an effective disinfection protocol is advised. CDC (2018) recommended that all DUWLs should use water that meets the Environmental Protection Agency (EPA) regulatory standards for drinking water (i.e., ≤ 500 CFU/mL of heterotrophic water bacteria).

Studies that examined ways to optimize capture efficiency of aerosols and droplets shields are scarce. This current study assessed the ability of the prototype aerosol containment device collaboratively developed by the University of Oklahoma Health Sciences Center College of Dentistry (OUCOD) and the Tom Love Innovation Hub at the University of Oklahoma (OU) to effectively capture smaller aerosol particles at varied extraction flow rates and interception positions relative to the emission source. This study is considered as an essential prerequisite before a clinical validation of the ProTecT-Shield (PTS).

Problem Statement

Studies that examine the capture efficiencies of high-volume evacuation systems for dental applications at varied flow rates and distances are rare. Dental aerosols are mixtures of water, blood, saliva, mineralized tissues, dental biomaterials, and other fluids from the oral cavity. Several studies have reported on the potential for contamination and airborne disease transmission as a result of aerosol generated by high-speed rotary instruments during routine dental treatments. PTS is a prototype aerosol containment device that is being currently used by faculty, students, and staff at the clinics of the University of Oklahoma Health Sciences Center College of Dentistry, Children's Hospital, OUCOD remote sites in Oklahoma

(Ardmore, Bartlesville, and Weatherford), Catholic charities and the Good Shepperd. According to a previous study from our group, PTS has the potential to reduce the concentration of airborne particles in a dental clinic simulation. Despite the promising results reported, the study did not assess the capture efficiency of PTS at varied geometry and flow rates, rather it focused on the reduction of aerosol throughout an open floor plan clinic when PTS was used in a single configuration. This present study was focused on comprehensively determining the efficiency of the PTS for capturing smaller aerosol particles at varied size ranges, air flow rates, plume velocities, and PTS vertical or upright positioning relative to the emission source.

Purpose and Scope

Studies to determine the efficiency of aerosol containment devices to capture particles in aerosols and minimize the transmission of airborne infectious respiratory diseases have not been rigorously executed. The purpose of the present study was to systematically assess the performance of a prototype aerosol containment device (Pro-TecT-Shield) collaboratively developed by OUCOD and the Tom Love Innovation Hub. Aerosol collection efficiency was characterized for particles <0.3 - 5 μm diameter with the Pro-TecT-Shield suction flow rate at two flow rates, in a number of conditions to determine the protective capacity of the Pro-TecT-Shield device. This study is essential to inform the effective clinical use of PTS during AGDPs.

Specific Objectives

The present study evaluated (1) PTS aerosol capture efficiencies at distinct flow rates for particles <0.3 – 5 μm, (2) impact of aerosol plume velocity on PTS performance, and (3) effects of PTS placement relative to aerosol plume.

CHAPTER II

MATERIALS AND METHODS

Experimental Design

This study was performed in 2 phases. Phase 1 was used to determine reasonable test parameters based off of measurements obtained during clinical simulation. Phase 2 was a rigorous examination of the collection efficiency of the PTS across many different parameters that spanned the measurements from Phase 1.

In Phase 1, the suction flow of the HVE installed at OUCOD dental clinics were measured to determine a range of operations. HVE flowrates ranging from approximately 104 Lpm to 194 Lpm were measured at the Green Clinic. In addition, air velocity around the face during dental procedure was determined while simulating the execution of different dental procedures such as ultrasonic scaling and cavity preparation in the Green Clinic of OUCOD with the assistance of Dr. Esteban Florez. To ensure the assessment of worst-case scenarios, the maximum and minimum air speeds were recorded while using an ultrasonic scaler and a high-speed hand turbine. Plume velocities ranging from approximately 3 Ft/min to 62 Ft/min were measured during the simulation of ultrasonic scaling and cavity preparation activities. This range of air velocities demonstrates the highly variable and directional aspects of dental plumes. The background air velocity measurements at the Green Clinic were between 5 Ft/min to 12 Ft/min. After rough establishment of the HVE flowrates, background air velocity, and dental plume velocities with empirical measurements, the following values for HVE and plume velocity were selected for evaluation in this study. HVE flowrates of 0 Lpm, 100 Lpm and 200 Lpm. 0 Lpm will serve as the control conditions so that collection efficiency can be calculated at 100 and 200 Lpm. Plume velocities of 6 Ft/min, 25 Ft/min, 50 Ft/min, and 100 Ft/min were selected to span across the measured range of plume velocities during dental simulation.

In Phase 2, the capture efficiency for PTS was determined for particle size range of <0.3 µm to 5 µm in a controlled laboratory setting. In addition to measuring capture efficiency at the three HVE flowrates and four dental plume velocities noted above, nine different spatial positionings of PTS were evaluated as well (Figure 3).

Columns are
7.62 cm apart

Figure 3: Experimental setup showing plume locations columns

In all conditions, the PTS was positioned 13 cm above the plume source as selected by Dr. Esteban Florez. This distance was selected because the PTS is currently used at a vertical height of ~13 cm during dental procedures at the Green Clinic of OUCOD and this height provides sufficient room for access to the patient's mouth. The same sodium chloride (NaCl) challenge aerosol used to evaluate respirator filtration efficiency was used in this study and is described in detail below. For this study, a field portable aerosol instrument was used to measure particle capture between <0.3 µm up to 20 µm since this particle size range is of greatest concern for the transmission of airborne infectious respiratory diseases and this type of instrument can easily be used in the field to verify the performance of PTS during clinical activities.

Materials

The materials used to perform this study included: GRIMM Portable Aerosol Spectrometer (Model 101) which was used to measure aerosol particle counts at different sizes. TSI Anemometer (Model 9515) was used to measure the air velocities in the dental clinic simulation and the laboratory experiment. A high-volume vacuum source (ShopVac, 6 hp, 20 gallon) was used to generate suction flow through the PTS in place of a dental HVE system. The ShopVac was powered through a variable voltage transformer to adjust suction airflow to the desired points (100 and 200 Lpm). A protect shield was provided by the OUCOD for evaluation in this project. A Collison 3-Jet Nebulizer (3 Jet, CH Technologies, Westwood NJ, USA) was used to generate the challenge aerosol. A pressure / vacuum pump (Model S55JXTJN8535) was at approximately 15 psi to power the nebulizer. A second pressure / vacuum pump was used to make up the total flow to10 Lpm. Aerosol flow was directed through ¾ inch copper plumbing through a manikin head to the oral cavity. Various copper and stainless-steel connectors of varied diameter were used to control the aerosol plume exit velocity.

Aerosol Generation

The test aerosol was generated from a 2% NaCl solution nebulized by a Collision Nebulizer at approximately 15 pounds per square inch (psi) (Cai and Floyd, 2020; NIOSH, 2019). This produces a Polydispersed aerosol with particle sizes ranging from 10 nm up to ~5 μm, with mean particle size distributions ~70 nm and geometric standard deviation of <1.87. The test aerosol was combined into a HEPA filtered air stream for a total flowrate of 10 Lpm (+/-0.1 Lpm).

Aerosol Plume Velocity

Plume velocities were produced in the laboratory at each of the four levels based on the velocities determined in Phase 1. These aerosol plume velocities were 6, 25, 50, and 100 Ft/min. Aerosol was delivered through 3/4th inch copper pipe into the manikin head at a constant flow rate. The desired exit velocity was obtained by sizing the aerosol outlet. At 10 Lpm flow rate, the plume velocity of 3/4th inch copper pipe produced 100 Ft/min. Through a ¾ inch to 1 inch copper coupling the flow rate was 50 Ft/min. Through a

3/4th inch to 1.5-inch coupling the flow rate was 25 Ft/min. Adapting the ¾ inch copper pipe to a 4-inch metal funnel produce 6 Ft/min plume velocity.

Aerosol Measurement

The centerline of the aerosol plume was determined, and PTS was placed at a vertical height of 13 cm from the aerosol source. The shield portion of the PTS was divided into nine (9) zones uniformly dividing the surface of the shield. Each location was marked in the center of the zone with a number from 1 – 9. The locations marked on the middle, left, right of the transparent shield were each measured at 3, 7 and 11 cm away from the suction manifold and each column was 7.62 cm apart from the center of the shield, as shown below in Figure 3.

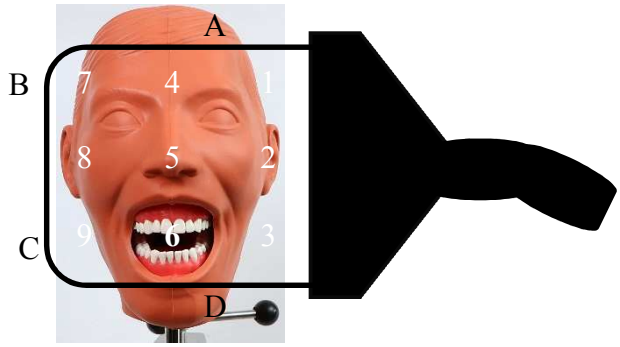

Figure 4: Top view illustration of aerosol plume focused on location 6.
Image source: TJIRIS Dental Education

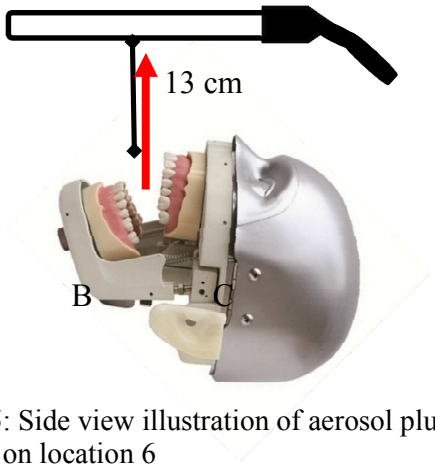

Figure 5: Side view illustration of aerosol plume focused on location 6
Image source: Dentalhonest

Aerosol plume of known velocities generated by the nebulizer was ejected through stainless-steel fitting and copper couplings fittings with known diameter. The aerosol plume centerline was directed at each of the marked locations on the shield at each study design plume velocity.

To measure the collection efficiency of the PTS, the GRIMM sampling probe was positioned at four points (A, B, C and D) around the edge of the shield with 10 aerosol count measurements collected at each location. Particles intercepted by the shield and failed to be captured tend to escape, therefore, these four locations along the perimeter of the shield were selected to measure particles that were not captured.

The mean count concentration for each particle size was calculated from the data collected at points A, B, C and D. Systematic aerosol measurements were collected in the same order for each of the possible plume velocity and shield location combinations starting with HVE flowrate at 0 Lpm (control condition), then at 100 Lpm, and finally at 200 Lpm. The aerosol measurements collected without the HVE suction were used as the reference values when estimating aerosol collection efficiency at the HVE flowrates of 100 Lpm and 200 Lpm. The average capture efficiency for each experimental configuration was calculated for each of the available size-bins reported by the GRIMM.

The collection efficiency at 100 Lpm was calculated using the formula below:

$$\frac{Average\ particle\ count\ @each\ size\ bin\ @zero\ Lpm - Average\ particle\ count\ @each\ size\ bin\ @100\ Lpm}{Average\ particle\ count\ @each\ particle\ size\ bin\ @zero\ Lpm}$$

The collection efficiency at 200 Lpm was calculated using the formula below:

$$\frac{Average\ particle\ count\ @each\ size\ bin\ @zero\ Lpm - Average\ particle\ count\ @each\ size\ bin\ @100\ Lpm}{Average\ particle\ count\ @each\ particle\ size\ bin\ @zero\ Lpm}$$

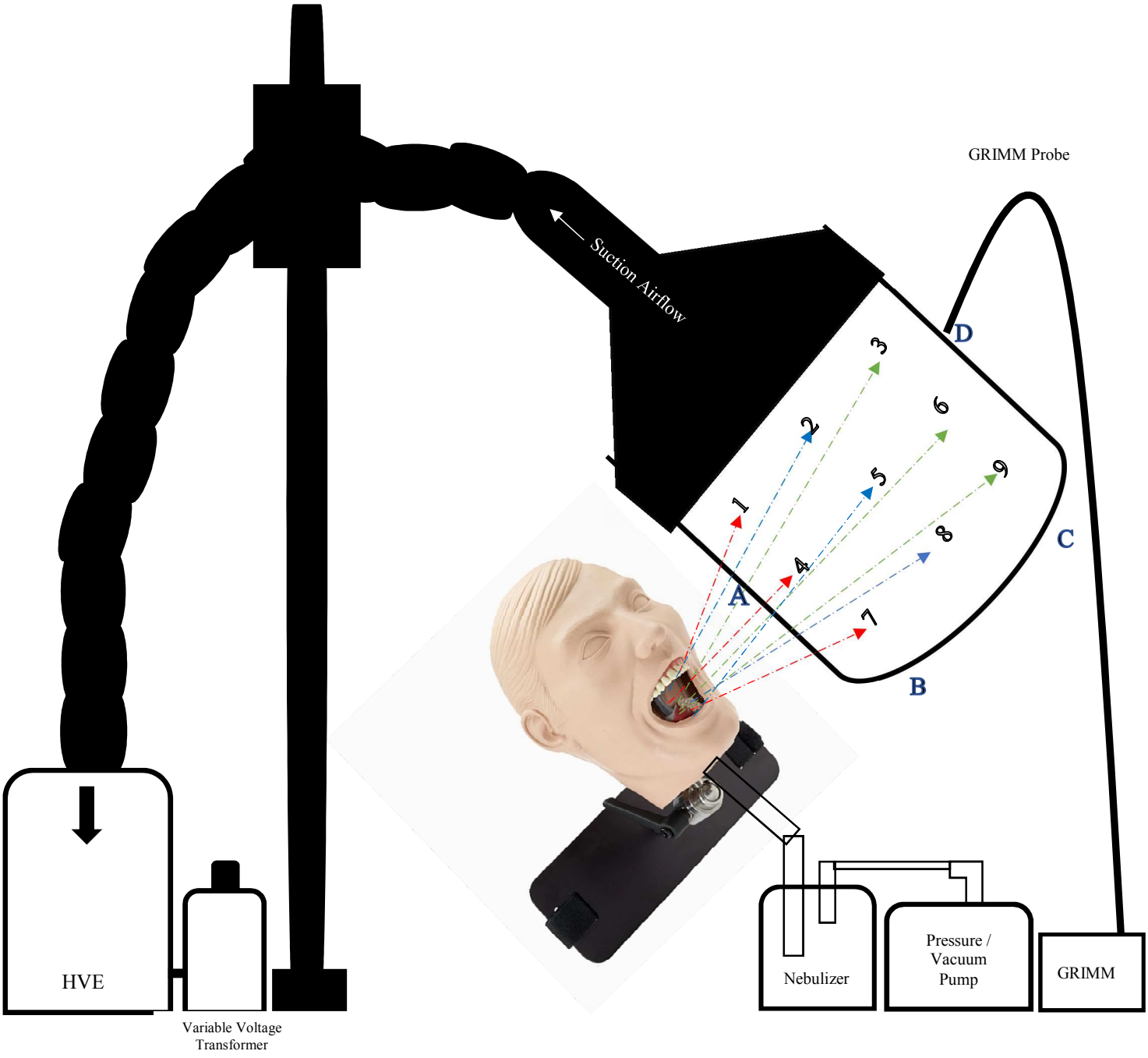

Figure 6: Graphical Representation of Laboratory Experimental Setup

Aerosol Spectrometer

The aerosol spectrometer, also known as GRIMM is a compact portable device which have been built for continuous measurement of airborne particles as well as for measuring the particle count distribution. The data from the device was reported as mass concentration in the unit microgram per cubic meter (μg/m3), assuming unit density of aerosol particles. The particle mass fractions were calculated by the GRIMM software and reported in occupational health terms: inhalable, thoracic and alveolic fractions. The measuring principle of the GRIMM is the light scattering of single particles with a semiconductor laser as light source. Inside the measuring cell the scattering light is being led directly and via a mirror with a wide opening angle onto the detector. The detector is positioned in the right angle to the incident laser beam. This setup of the detector is denominated as 90° scattering light detection. This optical alignment increases the scattering light collected by the detector and optimizes the signal-to-noise ratio. Therefore, particle sizes as small as 0.1 μm can be detected, but the smallest bin-size reported by the GRIMM is "<0.3".

HVE Flowrates and Plume Velocities

This study was conducted at two different flow rates indexed on the flow rate measurements of the HVE system installed in the dental clinics of the OUCOD. The maximum HVE flowrate measured at the Green Clinic was approximately 194 Lpm. To assess PTS capture efficiencies at low and high HVE flowrates, 0 Lpm, 100 Lpm and 200 Lpm were used for this simulation. Aerosol plume was generated at a constant flowrate of 10 Lpm. At HVE flowrate of 0 Lpm, aerosol capture efficiency for each of the 9 locations marked on the shield were assessed at each of the six plume velocities (i.e., 6 Ft/min, 25 Ft/min, 50 Ft/min, 100 Ft/min). As shown in Figure 6, the aerosol plume centerline was positioned at each of the 9 locations and aerosol measurements were collected from four locations (A, B, C, D) around the edges shield of the PTS using the GRIMM Aerosol Spectrometer.

Figure 7: Laboratory Experimental Setup

Data Analysis

As briefly noted above, the arithmetic means of particle count measurements obtained from points A, B, C, and D around the edges of the shield were calculated during each test condition and used to calculate an overall capture efficiency by comparing the mean particle counts with no HVE flow to the corresponding test with HVE flow. Since the overall capture efficiency of the PTS was the main interest in this study and particle count observations from four distinct points around the shield were used to make this assessment, the arithmetic mean of particle counts was used. Additionally, since each mean was calculated from 40 data points, the central limit theorem was applied to satisfy assumption of normality of particle count distribution. Initial data cleaning was conducted manually by selecting the 10 particle count measurements collected at each probe location for each trial. The cleaned data was assembled into a single spreadsheet and imported into a custom Python code developed by Dr. Cai. The Python code calculated the collection efficiency of each experimental conditions one size-bin at a time and performed the statistical analysis on the calculated collection efficiencies. The overall PTS collection efficiency for each of the unique experimental conditions was calculated from the difference in mean particle counts at 0 Lpm and 100 or 200 Lpm for the corresponding experimental condition. Plots and heat maps were constructed for

particle size bins and plume locations at each plume velocity to visualize the trends and variations in the collection efficiencies by HVE flowrates, plume velocities, and plume locations. In addition, statistical comparisons across flowrates, plume velocities and plume locations were made with a linear mixed effect model using Python. The main effects (independent variables) were HVE flowrate and plume location. Plume velocity is also an independent variable, but was modeled as a random effect since in a real clinical setting this factor would be poorly controlled and randomly encountered as various tools are used for various procedures. The independent variables were carefully controlled within the laboratory and with use of the mixed effects regression model, collection efficiency (dependent variable) of PTS was predicted. This model assumes normality of data and this assumption was satisfied with the using the central limit theorem due to the large dataset. Lastly, it should be noted that zero count values were obtained for particle size bins greater than 5 μm, therefore PTS collection efficiency was calculated for particle size bins 5 μm and below. This was due to the selected challenge aerosol which does not produce large particles.

CHAPTER III

RESULTS

Complete experimental data for the overall average collection efficiencies for each particle size bin (i.e., <0.3 μm to 5 μm) are presented in Appendix A. To simplify visual understanding of the data, particle size-bin collection efficiency data was grouped into three ranges. The size ranges are <0.30 μm – 0.65 μm, 0.80 μm – 1.60 μm, and 2.0 μm – 5.0 μm. Illustrations of these data are presented in Figures 8 – 17, below. Figures 8 - 17 represent PTS showing the suction airflow direction and plume locations 1-9. The three collection efficiencies at each of the plume locations 1-9 are the average collection efficiencies for the particle size bins listed on the left end of the shield. Since alveolic fraction represents particles under ~4 μm, it can be used as a proxy for overall collection efficiency as observed in this study. These data are shown in figures 14 – 15. The statistical analysis data for particle count values and alveolic fraction showing HVE flowrate and plume location as the main effects are presented Figure 16-17.

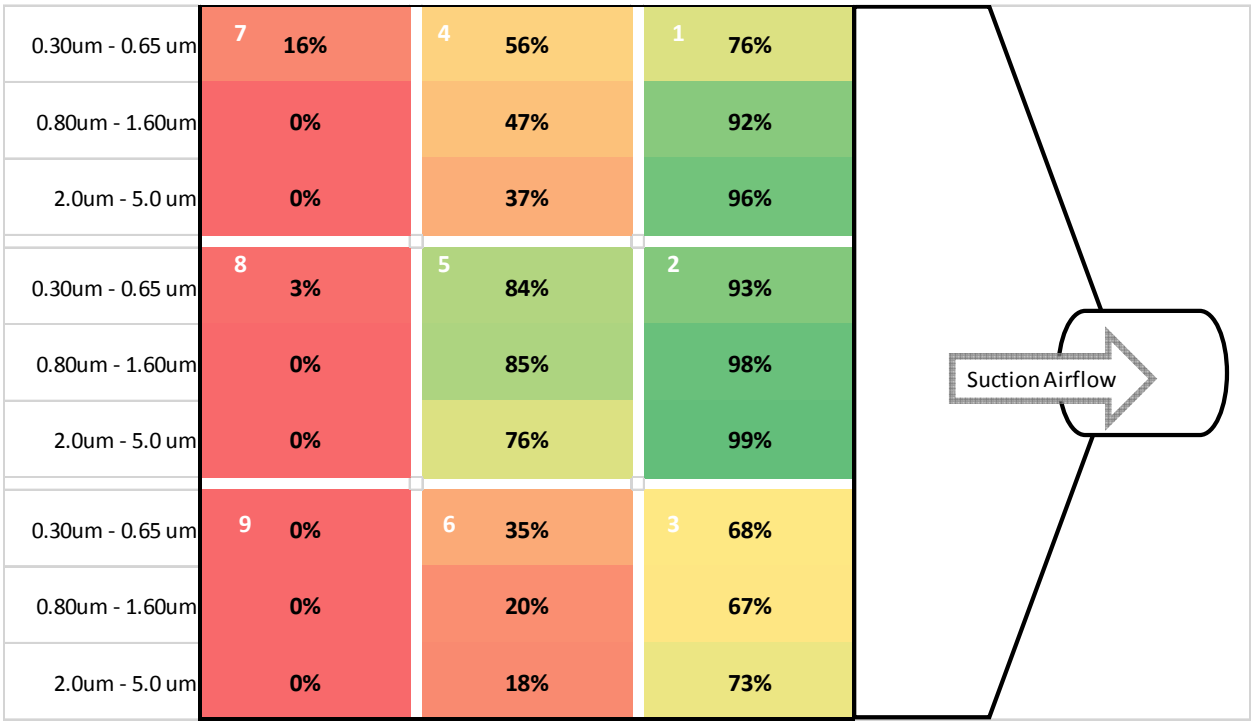

Figure 8: Collection efficiencies at 100 Lpm with plume velocity at 100 Ft/min.

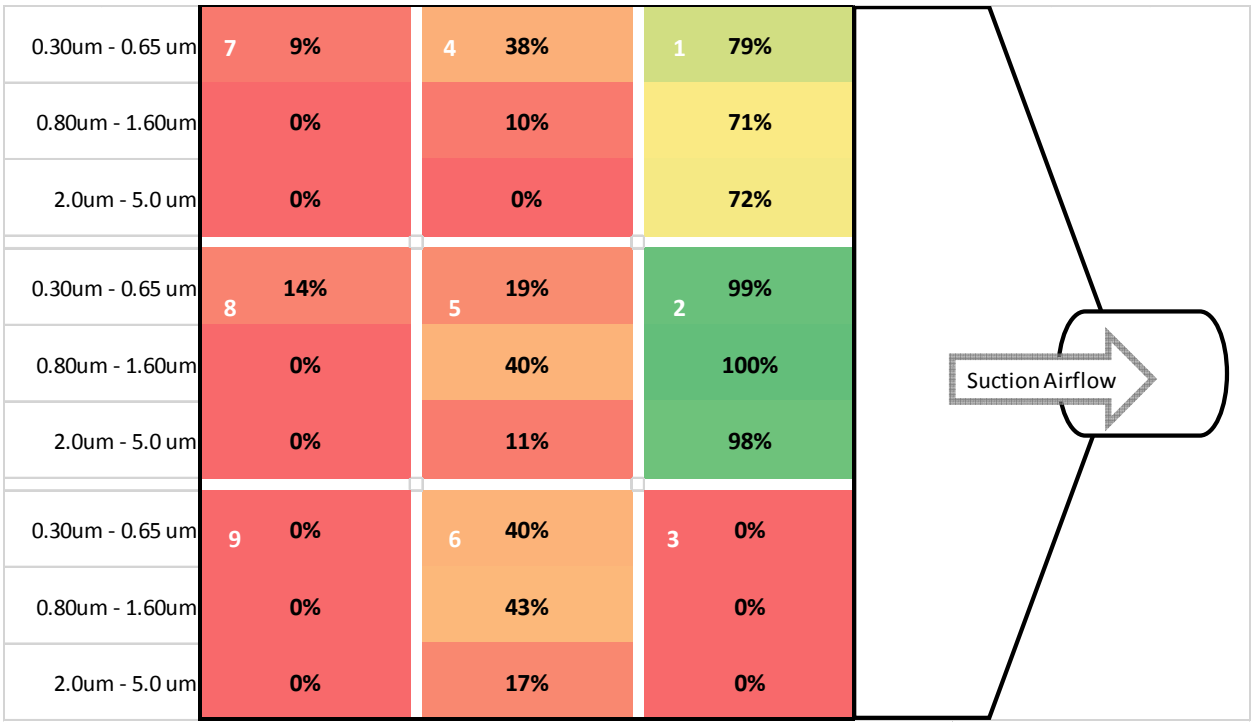

Figure 9: Collection efficiencies at 100 Lpm with plume velocity at 50 Ft/min.

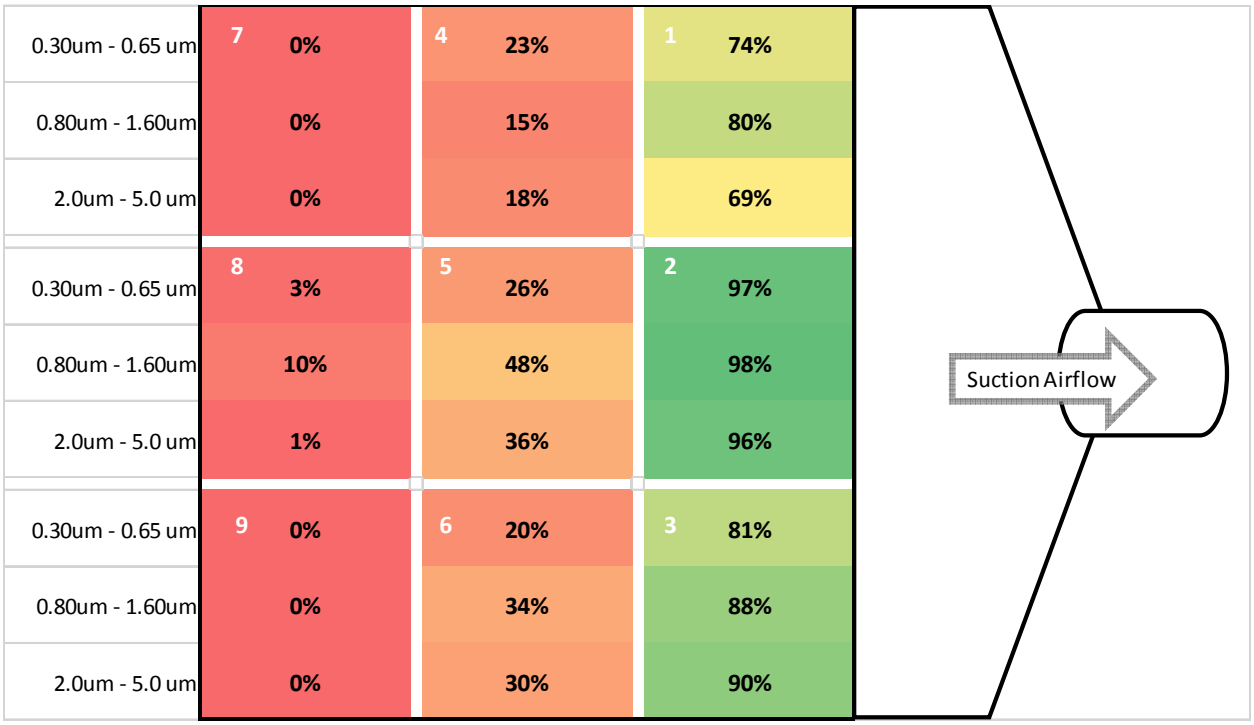

Figure 10: Collection efficiencies at 100 Lpm with plume velocity at 25 Ft/min.

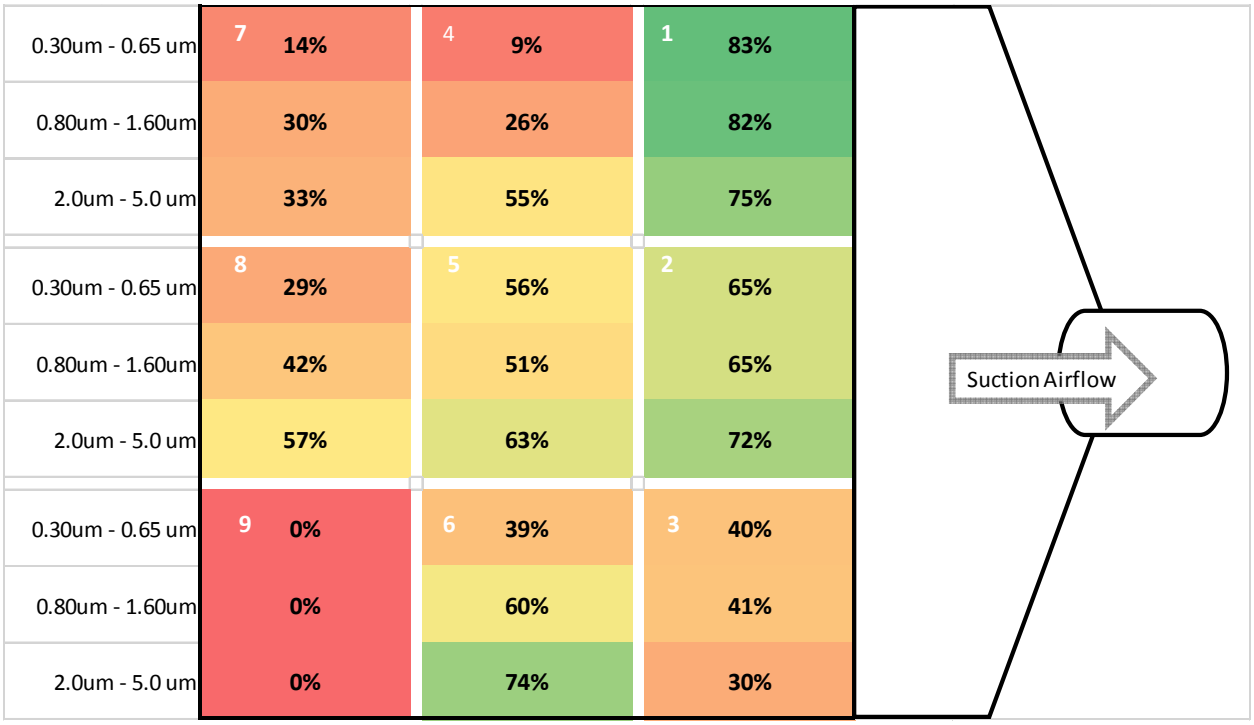

Figure 11: Collection efficiencies at 100 Lpm with plume velocity at 6 Ft/min.

At a flowrate of 100 Lpm and the four plume velocities, collection efficiencies decrease as the distance from the PTS suction manifold increased. Overall, plume locations 1-3 had higher collection efficiencies, followed by plume locations 4-6, and plume locations 7-9 had lowest and overall, quite poor collection efficiencies for all particle sizes measured in this study (0.30 – 5.0 μm).

Figures 13-16 below show the collection efficiencies for PTS at 200 Lpm. Collection efficiency was higher for all plume velocities and all measured partible sizes (0.3 μm to 5.0 μm). The overall acceptable collection efficiency consistently observed at plume locations 1-6 was 71-100%. However, at HVE flowrate of 200 Lpm and plume velocities of 25 Ft/min and 6 Ft/min, collection efficiencies within an acceptable range of 70-95% were observed at plume locations 7-9. (Figure 14-15).

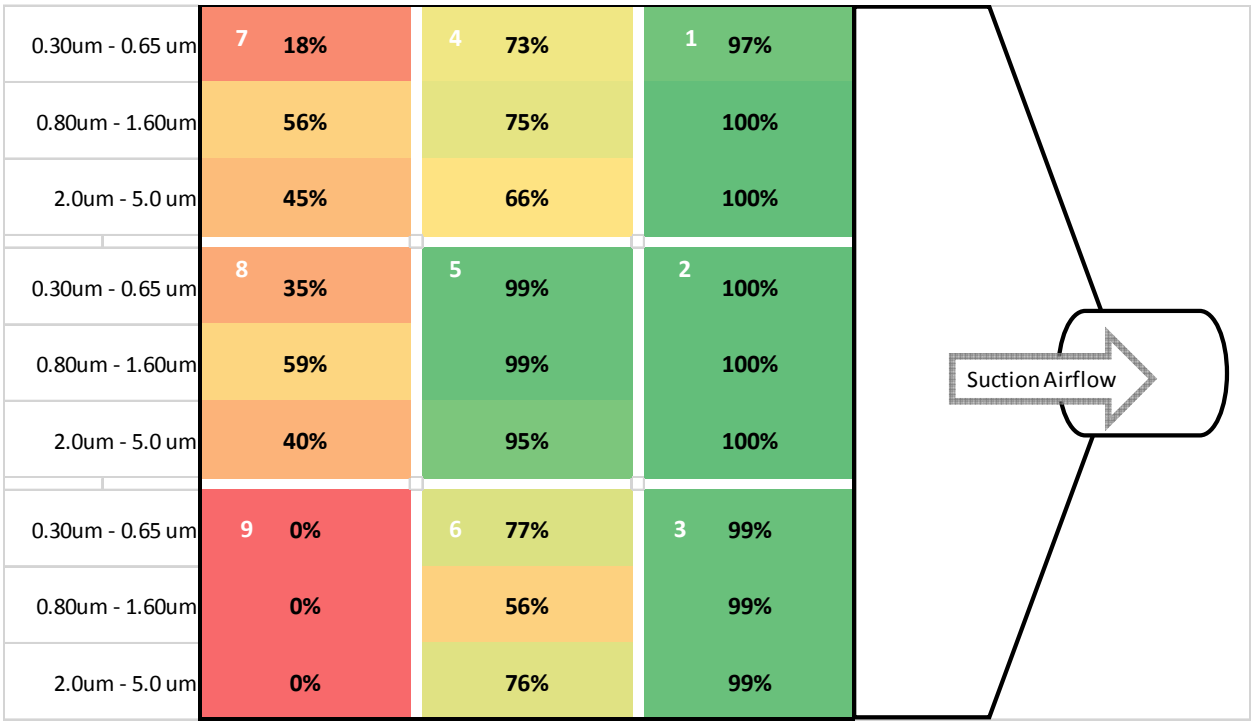

Figure 12: Collection efficiencies at 200 Lpm with plume velocity at 100 Ft/min.

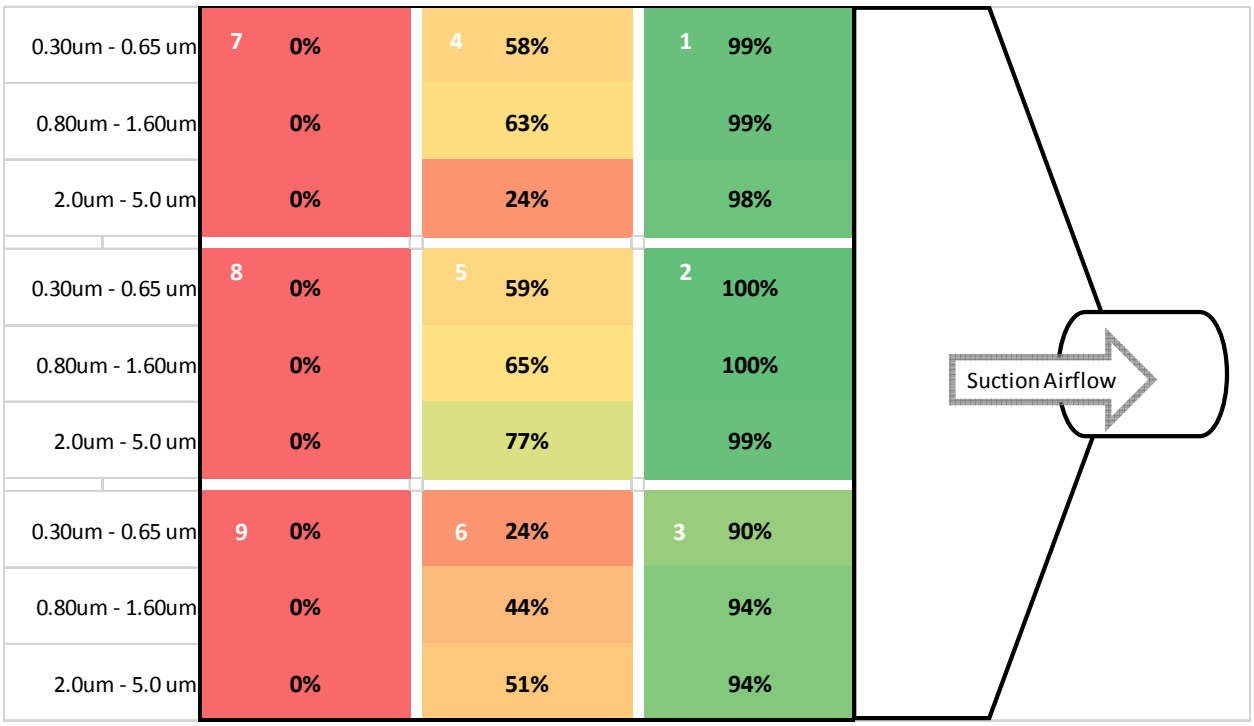

Figure 13: Collection efficiencies at 200 Lpm with plume velocity at 50 Ft/min.

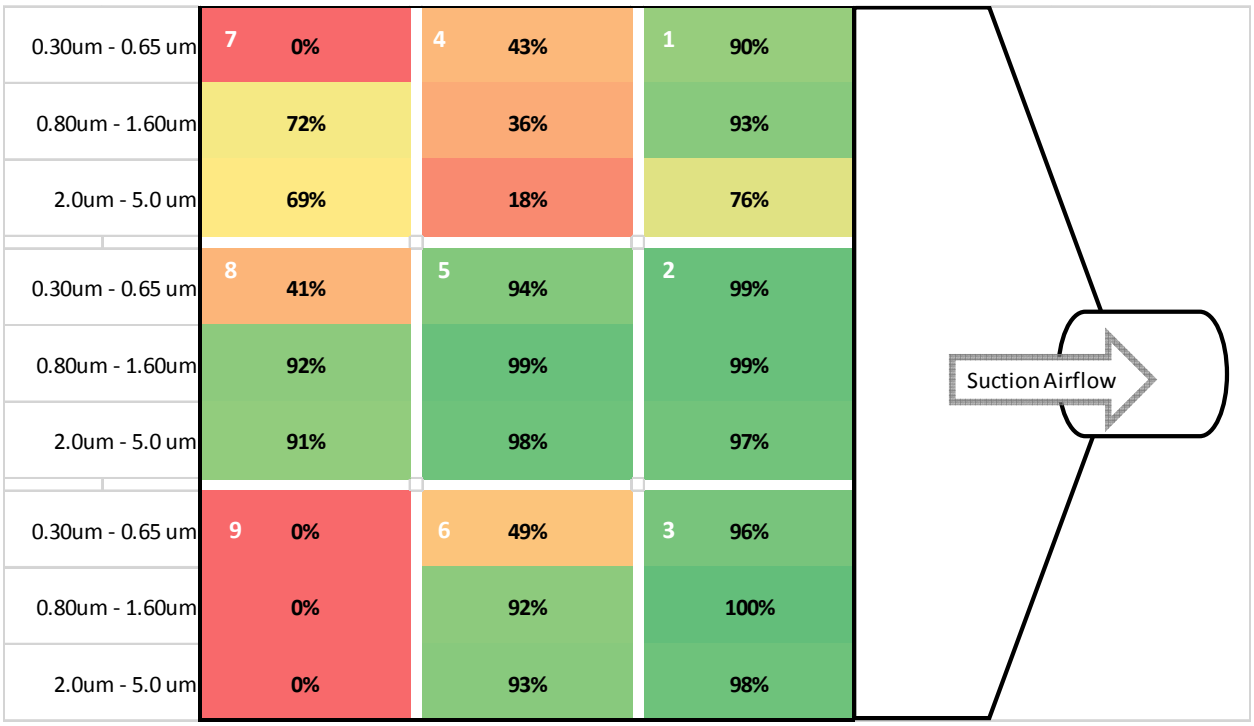

Figure 14: Collection efficiencies at 200 Lpm with plume velocity at 25 Ft/min.

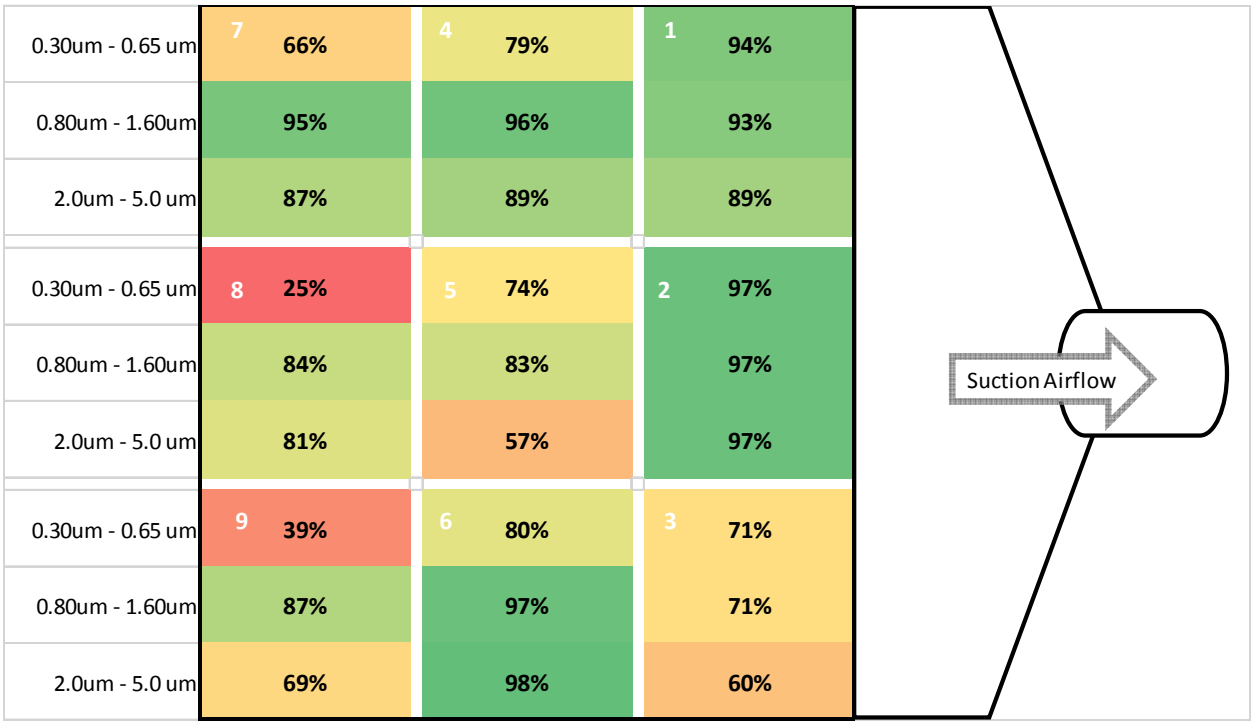

Figure 15: Collection efficiencies at 200 Lpm with plume velocity at 6 Ft/min.

The collection efficiencies of the alveolic particles at each of the nine plume locations are shown below.

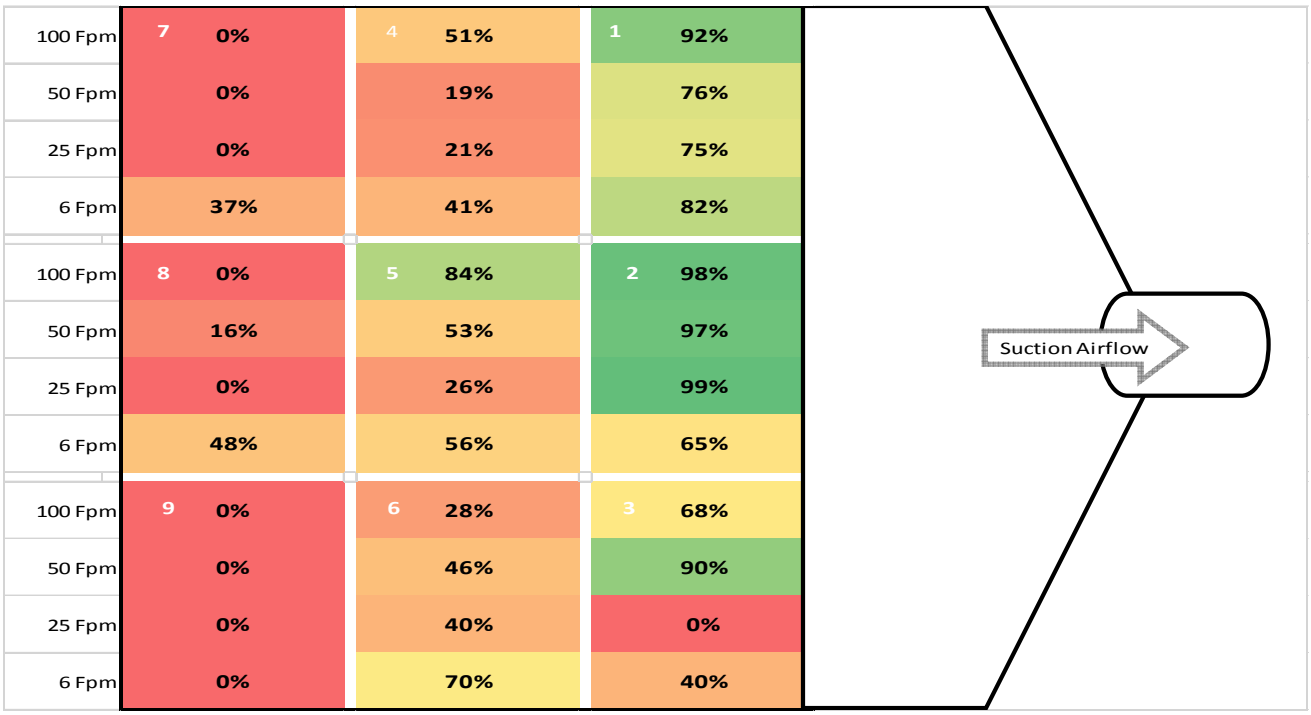

Figure 16: Collection efficiencies at 100 Lpm. for alveolic particles at varied plume velocities

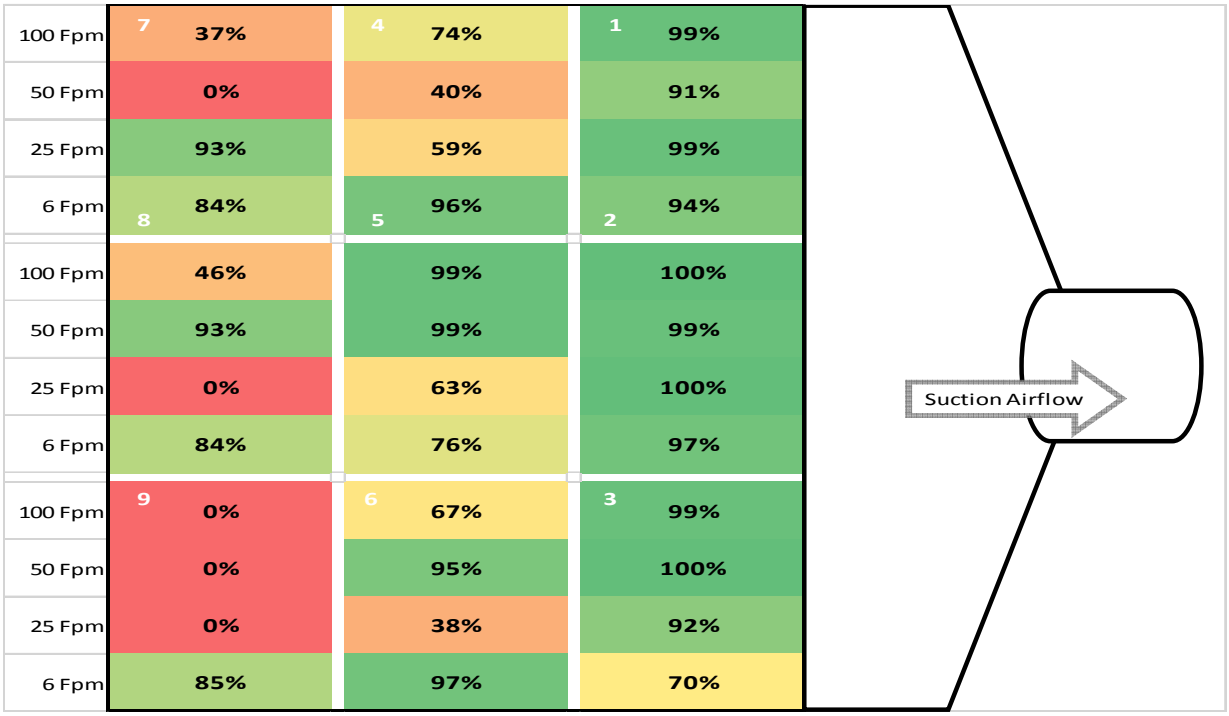

Figure 17: Collection efficiencies at 200 Lpm for alveolic fraction at varied plume velocities

Statistical Analysis Data

A mixed effects linear regression model was used for the statistical analysis of this complex dataset. The model contains both main effects and random effects. Main effects (i.e., HVE flowrates and plume locations) assumes that the individual specific effect is correlated to the independent variables. The group variable is modeled as a random effect (i.e., it assumes individual specific effect are not correlated with the independent variables. R-squared (R^2) is the proportion of total variability in the outcome that can be explained by the model. The regression coefficient values show how PTS collection efficiencies for plume locations 2-9 compares with location 1 which was selected by the model as the referent and is the intercept value. The range of R^2 was 0.65 to 0.74 with a trend of highest correlations at particle sizes 0.3 µm and 5.0 µm (Figure 18). According to the data below (Figure 18-30), the coefficients for locations 2, 3, and 5 were not significant in most model outputs, but the coefficients for locations 4, 6, 7, 8, and 9 were consistently significant. It should be noted that all particle size bin values are referred by the upper range value. For example, the 0.3 um size bin is actually particles less than 0.3 µm and 0.4 µm size means particles between 0.3 µm and 0.4 µm.

	Particle Count Size Bin (Plume Location 2-9)										
	0.30 um	0.40 um	0.50 um	0.65 um	0.80 um	1.0 um	1.60 um	2.0 um	3.0 um	4.0 um	5.0 um
Regression Cofficient For Intercept (Plume Location 1)	0.72	0.676	0.643	0.504	0.445	0.355	0.285	0.2	0.117	0.19	0.388
Regression Coefficient For Plume Location 2-9	-1.164 - 0.076	-1.181 - 0.075	-1.235 - 0.073	-1.474 - 0.061	-1.743 - 0.054	-1.841 - 0.060	-2.157 - 0.064	-2.424 - 0.063	-2.611 - 0.117	-2.355 - 0.118	-2.078 - 0.132
P-value For Intercept (Plume Location 1)	0.00	0.00	0.00	0.01	0.10	0.20	0.42	0.61	0.77	0.56	0.15
Plume Location with Significant P-values	4, 6, 7, 8, 9	4, 6, 7, 8, 9	4, 6, 7, 8, 9	4, 6, 7, 8, 9	7, 8, 9	7, 8, 9	7, 8, 9	7, 8, 9	7, 8, 9	7, 8, 9	4, 7, 8, 9
Regression Coefficient For HVE Flowrate	0.001	0.001	0.001	0.003	0.003	0.004	0.004	0.005	0.005	0.004	0.003
Regression Coefficient For Group Variable	0.008	0.009	0.012	0.034	0.083	0.072	0.141	0.174	0.213	0.136	0.074
R-Square	0.714	0.708	0.69	0.706	0.677	0.674	0.659	0.66	0.705	0.733	0.747

Figure 18: Summary Data analysis output for particle count values

Mixed Linear Model Regression Results For 0.3 um Particle

Model:	MixedLM	Dependent Variable:	col_eff
No. Observations:	72	Method:	REML
No. Groups:	4	Scale:	0.0742
Min. group size:	18	Log-Likelihood:	-24.3625
Max. group size:	18	Converged:	Yes
Mean group size:	18.0		

	Coef.	Std.Err.	z	P>|z|	[0.025	0.975]
Intercept	0.720	0.143	5.020	0.000	0.439	1.001
jet_location[T.l_2]	0.076	0.136	0.555	0.579	-0.191	0.342
jet_location[T.l_3]	-0.166	0.136	-1.219	0.223	-0.433	0.101
jet_location[T.l_4]	-0.364	0.136	-2.673	0.008	-0.631	-0.097
jet_location[T.l_5]	-0.227	0.136	-1.667	0.096	-0.494	0.040
jet_location[T.l_6]	-0.382	0.136	-2.809	0.005	-0.649	-0.116
jet_location[T.l_7]	-0.774	0.136	-5.686	0.000	-1.041	-0.507
jet_location[T.l_8]	-0.721	0.136	-5.296	0.000	-0.988	-0.454
jet_location[T.l_9]	-1.164	0.136	-8.551	0.000	-1.431	-0.897
flowrate	0.001	0.001	1.451	0.147	-0.000	0.002
Group Var	0.008	0.037				

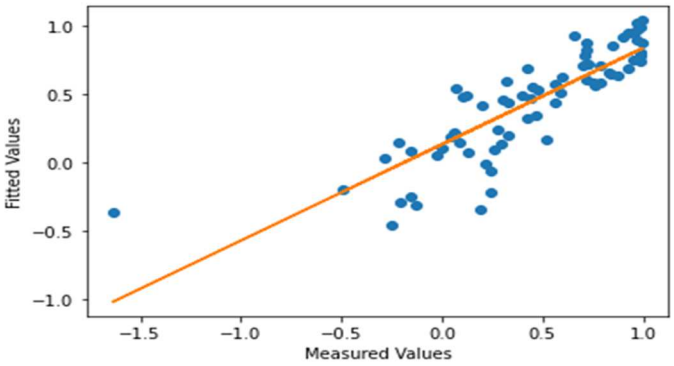

R^2 = 0.7141675147940397

Figure 19: Flowrate and plume location interaction for < 0.30 µm particle size bin

Mixed Linear Model Regression Results For 0.4 um Particle

Model:	MixedLM	Dependent Variable:	col_eff
No. Observations:	72	Method:	REML
No. Groups:	4	Scale:	0.0778
Min. group size:	18	Log-Likelihood:	-25.9188
Max. group size:	18	Converged:	Yes
Mean group size:	18.0		

	Coef.	Std.Err.	z	P>|z|	[0.025	0.975]
Intercept	0.676	0.147	4.587	0.000	0.387	0.965
jet_location[T.l_2]	0.075	0.139	0.537	0.591	-0.198	0.348
jet_location[T.l_3]	-0.183	0.139	-1.311	0.190	-0.456	0.090
jet_location[T.l_4]	-0.379	0.139	-2.720	0.007	-0.653	-0.106
jet_location[T.l_5]	-0.243	0.139	-1.744	0.081	-0.517	0.030
jet_location[T.l_6]	-0.395	0.139	-2.832	0.005	-0.668	-0.122
jet_location[T.l_7]	-0.762	0.139	-5.462	0.000	-1.035	-0.488
jet_location[T.l_8]	-0.717	0.139	-5.143	0.000	-0.991	-0.444
jet_location[T.l_9]	-1.186	0.139	-8.506	0.000	-1.460	-0.913
flowrate	0.001	0.001	1.816	0.069	-0.000	0.002
Group Var	0.009	0.040				

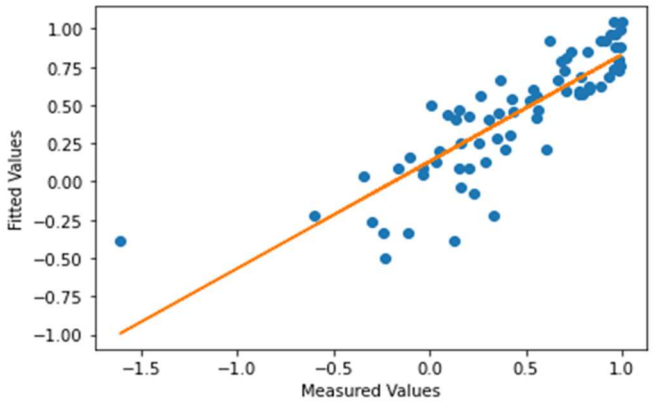

R^2 = 0.7084351069289714

Figure 20: Flowrate and plume location interaction for < 0.4 µm particle size bin

Mixed Linear Model Regression Results For 0.5 um Particle

Model:	MixedLM	Dependent Variable:	col_eff
No. Observations:	72	Method:	REML
No. Groups:	4	Scale:	0.0966
Min. group size:	18	Log-Likelihood:	-32.6679
Max. group size:	18	Converged:	Yes
Mean group size:	18.0		

	Coef.	Std.Err.	z	P>|z|	[0.025	0.975]
Intercept	0.643	0.165	3.911	0.000	0.321	0.966
jet_location[T.l_2]	0.073	0.155	0.470	0.638	-0.232	0.378
jet_location[T.l_3]	-0.199	0.155	-1.282	0.200	-0.504	0.105
jet_location[T.l_4]	-0.415	0.155	-2.668	0.008	-0.719	-0.110
jet_location[T.l_5]	-0.248	0.155	-1.596	0.111	-0.553	0.057
jet_location[T.l_6]	-0.495	0.155	-3.187	0.001	-0.800	-0.191
jet_location[T.l_7]	-0.853	0.155	-5.486	0.000	-1.157	-0.548
jet_location[T.l_8]	-0.773	0.155	-4.971	0.000	-1.077	-0.468
jet_location[T.l_9]	-1.235	0.155	-7.946	0.000	-1.540	-0.930
flowrate	0.001	0.001	1.961	0.050	0.000	0.003
Group Var	0.012	0.046				

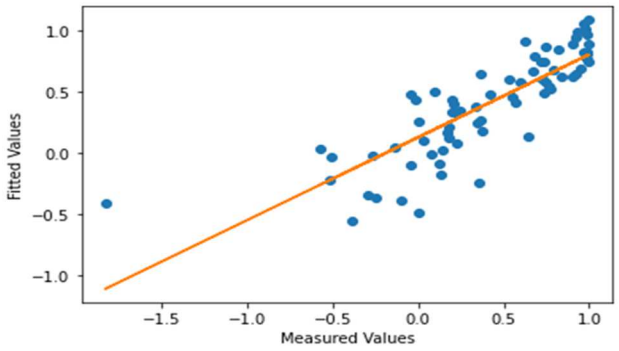

R^2 = 0.6903597697746962

Figure 21: Flowrate and plume location interaction for < 0.5 µm particle size bin

Mixed Linear Model Regression Results For 0.65 um Particle

Model:	MixedLM	Dependent Variable:	col_eff
No. Observations:	72	Method:	REML
No. Groups:	4	Scale:	0.1237
Min. group size:	18	Log-Likelihood:	-41.2519
Max. group size:	18	Converged:	Yes
Mean group size:	18.0		

	Coef.	Std.Err.	z	P>|z|	[0.025	0.975]
Intercept	0.504	0.198	2.541	0.011	0.115	0.893
jet_location[T.l_2]	0.061	0.176	0.345	0.730	-0.284	0.405
jet_location[T.l_3]	-0.197	0.176	-1.120	0.263	-0.541	0.148
jet_location[T.l_4]	-0.403	0.176	-2.291	0.022	-0.747	-0.058
jet_location[T.l_5]	-0.192	0.176	-1.090	0.275	-0.536	0.153
jet_location[T.l_6]	-0.374	0.176	-2.126	0.033	-0.718	-0.029
jet_location[T.l_7]	-0.802	0.176	-4.561	0.000	-1.147	-0.457
jet_location[T.l_8]	-0.611	0.176	-3.474	0.001	-0.955	-0.266
jet_location[T.l_9]	-1.474	0.176	-8.380	0.000	-1.818	-1.129
flowrate	0.003	0.001	3.079	0.002	0.001	0.004
Group Var	0.034	0.097				

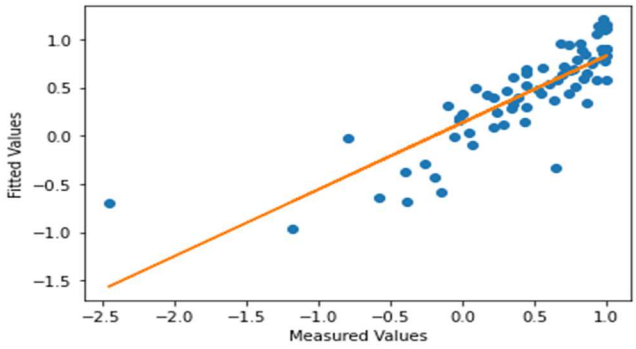

R^2 = 0.7062686053490885

Figure 22: Flowrate and plume location interaction for < 0.65 µm particle size bin

Mixed Linear Model Regression Results For 0.80 um Particle

Model:	MixedLM	Dependent Variable:	col_eff
No. Observations:	72	Method:	REML
No. Groups:	4	Scale:	0.2113
Min. group size:	18	Log-Likelihood:	-58.3162
Max. group size:	18	Converged:	Yes
Mean group size:	18.0		

	Coef.	Std.Err.	z	P>|z|	[0.025	0.975]
Intercept	0.445	0.271	1.642	0.101	-0.086	0.977
jet_location[T.l_2]	0.054	0.230	0.237	0.813	-0.396	0.505
jet_location[T.l_3]	-0.201	0.230	-0.874	0.382	-0.651	0.250
jet_location[T.l_4]	-0.379	0.230	-1.651	0.099	-0.830	0.071
jet_location[T.l_5]	-0.155	0.230	-0.676	0.499	-0.606	0.295
jet_location[T.l_6]	-0.271	0.230	-1.180	0.238	-0.722	0.179
jet_location[T.l_7]	-0.806	0.230	-3.509	0.000	-1.257	-0.356
jet_location[T.l_8]	-0.528	0.230	-2.297	0.022	-0.978	-0.077
jet_location[T.l_9]	-1.743	0.230	-7.583	0.000	-2.193	-1.292
flowrate	0.003	0.001	2.794	0.005	0.001	0.005
Group Var	0.083	0.172				

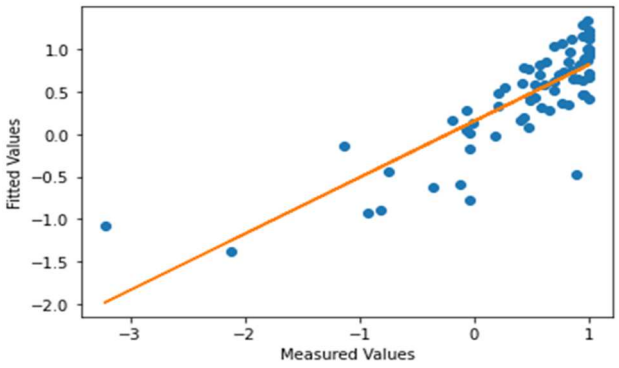

R^2 = 0.6766654665829459

Figure 23: Flowrate and plume location interaction for < 0.80 μm particle size bin

Mixed Linear Model Regression Results For 1.0 um Particle

Model:	MixedLM	Dependent Variable:	col_eff
No. Observations:	72	Method:	REML
No. Groups:	4	Scale:	0.2326
Min. group size:	18	Log-Likelihood:	-60.9872
Max. group size:	18	Converged:	Yes
Mean group size:	18.0		

	Coef.	Std.Err.	z	P>|z|	[0.025	0.975]
Intercept	0.355	0.276	1.286	0.199	-0.186	0.895
jet_location[T.l_2]	0.060	0.241	0.247	0.805	-0.413	0.532
jet_location[T.l_3]	-0.218	0.241	-0.905	0.366	-0.691	0.254
jet_location[T.l_4]	-0.452	0.241	-1.876	0.061	-0.925	0.020
jet_location[T.l_5]	-0.188	0.241	-0.779	0.436	-0.660	0.285
jet_location[T.l_6]	-0.402	0.241	-1.666	0.096	-0.874	0.071
jet_location[T.l_7]	-0.912	0.241	-3.783	0.000	-1.385	-0.440
jet_location[T.l_8]	-0.620	0.241	-2.572	0.010	-1.093	-0.148
jet_location[T.l_9]	-1.841	0.241	-7.634	0.000	-2.314	-1.368
flowrate	0.004	0.001	3.129	0.002	0.001	0.006
Group Var	0.072	0.147				

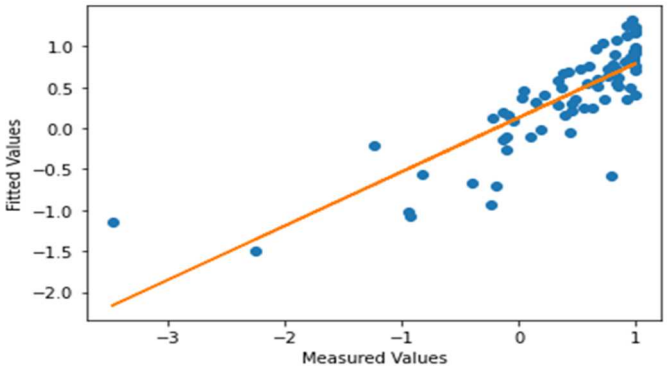

R^2 = 0.67413324964188

Figure 24: Flowrate and plume location interaction for < 1.0 μm particle size bin

Mixed Linear Model Regression Results For 1.60 um Particle

Model:	MixedLM	Dependent Variable:	col_eff
No. Observations:	72	Method:	REML
No. Groups:	4	Scale:	0.3596
Min. group size:	18	Log-Likelihood:	-74.8082
Max. group size:	18	Converged:	Yes
Mean group size:	18.0		

	Coef.	Std.Err.	z	P>|z|	[0.025	0.975]
Intercept	0.285	0.354	0.806	0.420	-0.408	0.979
jet_location[T.l_2]	0.064	0.300	0.213	0.831	-0.524	0.652
jet_location[T.l_3]	-0.227	0.300	-0.758	0.449	-0.815	0.361
jet_location[T.l_4]	-0.445	0.300	-1.485	0.138	-1.033	0.142
jet_location[T.l_5]	-0.176	0.300	-0.588	0.557	-0.764	0.412
jet_location[T.l_6]	-0.318	0.300	-1.060	0.289	-0.906	0.270
jet_location[T.l_7]	-0.958	0.300	-3.195	0.001	-1.546	-0.370
jet_location[T.l_8]	-0.590	0.300	-1.966	0.049	-1.177	-0.002
jet_location[T.l_9]	-2.157	0.300	-7.192	0.000	-2.744	-1.569
flowrate	0.004	0.001	2.770	0.006	0.001	0.007
Group Var	0.141	0.225				

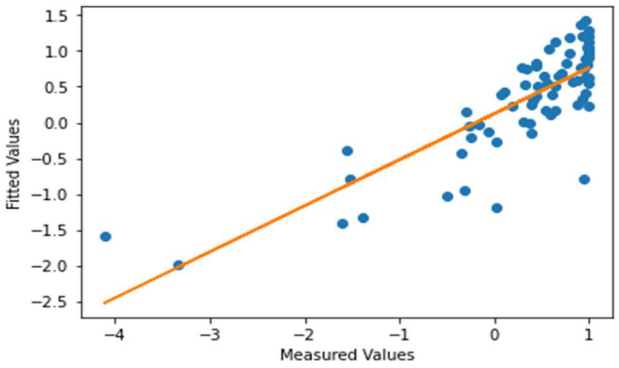

R^2 = 0.6586759050027144

Figure 25: Flowrate and plume location interaction for < 1.60 µm particle size bin

Mixed Linear Model Regression Results For 2.0 um Particle

Model:	MixedLM	Dependent Variable:	col_eff
No. Observations:	72	Method:	REML
No. Groups:	4	Scale:	0.4501
Min. group size:	18	Log-Likelihood:	-81.7445
Max. group size:	18	Converged:	Yes
Mean group size:	18.0		

	Coef.	Std.Err.	z	P>|z|	[0.025	0.975]
Intercept	0.200	0.395	0.506	0.613	-0.574	0.974
jet_location[T.l_2]	0.063	0.335	0.189	0.850	-0.594	0.721
jet_location[T.l_3]	-0.264	0.335	-0.787	0.431	-0.921	0.394
jet_location[T.l_4]	-0.443	0.335	-1.319	0.187	-1.100	0.215
jet_location[T.l_5]	-0.163	0.335	-0.485	0.628	-0.820	0.495
jet_location[T.l_6]	-0.250	0.335	-0.746	0.456	-0.908	0.407
jet_location[T.l_7]	-0.961	0.335	-2.865	0.004	-1.618	-0.304
jet_location[T.l_8]	-0.567	0.335	-1.690	0.091	-1.224	0.091
jet_location[T.l_9]	-2.424	0.335	-7.227	0.000	-3.082	-1.767
flowrate	0.005	0.002	2.873	0.004	0.001	0.008
Group Var	0.174	0.248				

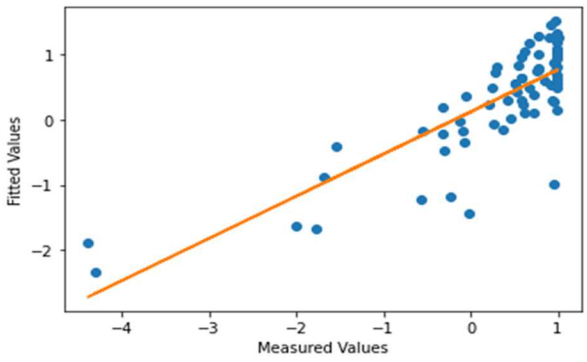

R^2 = 0.6598210288765665

Figure 26: Flowrate and plume location interaction for < 2.0 µm particle size bin

Mixed Linear Model Regression Results For 3.0 um Particle

Model:	MixedLM	Dependent Variable:	col_eff
No. Observations:	72	Method:	REML
No. Groups:	4	Scale:	0.4319
Min. group size:	18	Log-Likelihood:	-80.7884
Max. group size:	18	Converged:	Yes
Mean group size:	18.0		

	Coef.	Std.Err.	z	P>|z|	[0.025	0.975]
Intercept	0.117	0.401	0.292	0.770	-0.670	0.904
jet_location[T.l_2]	0.104	0.329	0.316	0.752	-0.540	0.748
jet_location[T.l_3]	-0.254	0.329	-0.772	0.440	-0.898	0.390
jet_location[T.l_4]	-0.471	0.329	-1.434	0.152	-1.115	0.173
jet_location[T.l_5]	-0.151	0.329	-0.461	0.645	-0.795	0.493
jet_location[T.l_6]	-0.247	0.329	-0.753	0.451	-0.891	0.397
jet_location[T.l_7]	-1.017	0.329	-3.095	0.002	-1.661	-0.373
jet_location[T.l_8]	-0.656	0.329	-1.997	0.046	-1.300	-0.012
jet_location[T.l_9]	-2.611	0.329	-7.948	0.000	-3.256	-1.967
flowrate	0.005	0.002	3.168	0.002	0.002	0.008
Group Var	0.213	0.302				

for < 3.0 µm particle size bin

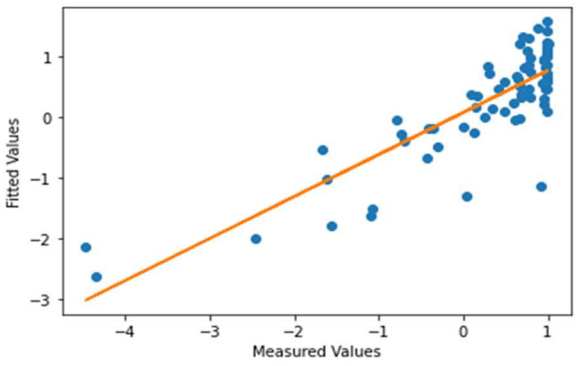

R^2 = 0.705338343093675

Figure 27: Flowrate and plume location interaction

Mixed Linear Model Regression Results For 4.0 um Particle

Model:	MixedLM	Dependent Variable:	col_eff
No. Observations:	72	Method:	REML
No. Groups:	4	Scale:	0.2960
Min. group size:	18	Log-Likelihood:	-68.9818
Max. group size:	18	Converged:	Yes
Mean group size:	18.0		

	Coef.	Std.Err.	z	P>|z|	[0.025	0.975]
Intercept	0.190	0.329	0.579	0.563	-0.454	0.834
jet_location[T.l_2]	0.118	0.272	0.435	0.663	-0.415	0.652
jet_location[T.l_3]	-0.206	0.272	-0.757	0.449	-0.739	0.327
jet_location[T.l_4]	-0.511	0.272	-1.880	0.060	-1.044	0.022
jet_location[T.l_5]	-0.238	0.272	-0.875	0.382	-0.771	0.295
jet_location[T.l_6]	-0.290	0.272	-1.066	0.287	-0.823	0.243
jet_location[T.l_7]	-1.101	0.272	-4.047	0.000	-1.634	-0.568
jet_location[T.l_8]	-0.676	0.272	-2.486	0.013	-1.210	-0.143
jet_location[T.l_9]	-2.355	0.272	-8.657	0.000	-2.888	-1.822
flowrate	0.004	0.001	3.328	0.001	0.002	0.007
Group Var	0.136	0.235				

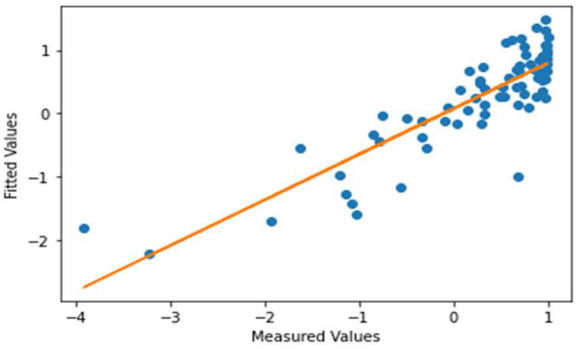

R^2 = 0.7330947370744922

Figure 28: Flowrate and plume location interaction for < 4.0 µm particle size bin

Mixed Linear Model Regression Results For 5.0 um Particle

Model:	MixedLM	Dependent Variable:	col_eff
No. Observations:	72	Method:	REML
No. Groups:	4	Scale:	0.2107
Min. group size:	18	Log-Likelihood:	-58.0919
Max. group size:	18	Converged:	Yes
Mean group size:	18.0		

	Coef.	Std.Err.	z	P>|z|	[0.025	0.975]
Intercept	0.388	0.267	1.454	0.146	-0.135	0.911
jet_location[T.l_2]	0.132	0.230	0.573	0.567	-0.318	0.581
jet_location[T.l_3]	-0.165	0.230	-0.721	0.471	-0.615	0.284
jet_location[T.l_4]	-0.536	0.230	-2.335	0.020	-0.986	-0.086
jet_location[T.l_5]	-0.258	0.230	-1.122	0.262	-0.707	0.192
jet_location[T.l_6]	-0.308	0.230	-1.341	0.180	-0.758	0.142
jet_location[T.l_7]	-1.221	0.230	-5.322	0.000	-1.671	-0.772
jet_location[T.l_8]	-0.726	0.230	-3.164	0.002	-1.176	-0.276
jet_location[T.l_9]	-2.078	0.230	-9.056	0.000	-2.528	-1.629
flowrate	0.003	0.001	2.585	0.010	0.001	0.005
Group Var	0.074	0.156				

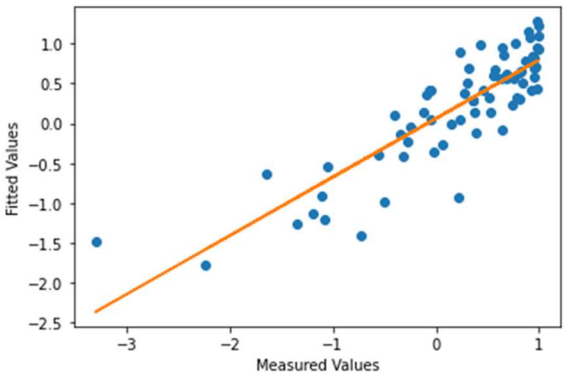

R2 = 0.7468683541793812

Figure 29: Flowrate and plume location interaction for < 5.0 µm particle size bin

Below is the statistical analysis output for < 0.3 µm – 5 µm particle size bin count values.

Mixed Linear Model Regression Results

Model:	MixedLM	Dependent Variable:	col_eff
No. Observations:	72	Method:	REML
No. Groups:	4	Scale:	0.1577
Min. group size:	18	Log-Likelihood:	-49.2867
Max. group size:	18	Converged:	Yes
Mean group size:	18.0		

	Coef.	Std.Err.	z	P>|z|	[0.025	0.975]
Intercept	0.461	0.235	1.961	0.050	0.000	0.922
jet_location[T.l_2]	0.059	0.199	0.298	0.766	-0.330	0.448
jet_location[T.l_3]	-0.208	0.199	-1.045	0.296	-0.597	0.182
jet_location[T.l_4]	-0.382	0.199	-1.925	0.054	-0.771	0.007
jet_location[T.l_5]	-0.190	0.199	-0.956	0.339	-0.579	0.199
jet_location[T.l_6]	-0.282	0.199	-1.418	0.156	-0.671	0.108
jet_location[T.l_7]	-0.760	0.199	-3.829	0.000	-1.149	-0.371
jet_location[T.l_8]	-0.558	0.199	-2.810	0.005	-0.947	-0.169
jet_location[T.l_9]	-1.634	0.199	-8.228	0.000	-2.023	-1.245
flowrate	0.003	0.001	3.019	0.003	0.001	0.005
Group Var	0.063	0.152				

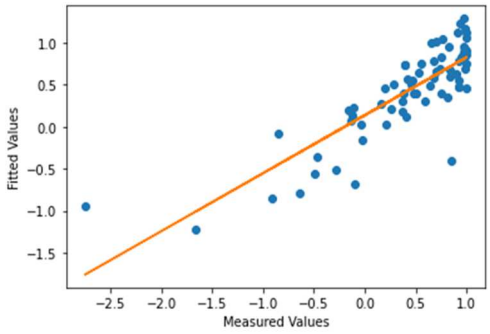

R2 = 0.7043847308490572

Figure 30: Flowrate and plume location interaction for alveolic particle

CHAPTER IV

DISCUSSION

Broad observations of PTS Collection Efficiency as influenced by Plume Location, Plume velocity and HVE flowrate

PTS collection efficiency varied based on HVE flowrate, plume location, and plume velocity. The most notable effect was observed in the HVE flow rate. In this study, collection efficiency of 70-100% is considered acceptable. Plume locations near the PTS suction manifold had higher collection efficiencies compared to locations further from the suction area of the shield. The overall collection efficiencies were consistently higher at plume locations closer to the PTS suction manifold at each of the plume velocities and HVE flowrates simulated. The effect of plume velocity was varied and specific conclusions cannot be made from this dataset. However, some broad observation can be made such as: very low plume velocity (6 Ftt/min, similar to that generated by ultrasonic scalers) has overall higher collection efficiency than high plume velocity (100 Ft/min, similar to turbine handpieces). The effect of plume velocity may have an unexplored interaction with the curved geometry of the PTS shield. As for particle sizes, moderate differences in PTS collection efficiencies based on particle size were observed for particles 0.30 μm – 5.0 μm, but these differences were not significant.

Effect of HVE Flowrates on PTS Collection Efficiency

As observed from this study, PTS had higher collection efficiency at HVE flowrate of 200 Lpm compared to 100 Lpm. The increase in collection efficiency between 100 and 200 Lpm was a significant difference as indicated by the P-value of 0.003 for HVE flowrate in the alveolic fraction model (Figure 30). At both HVE flowrates, overall collection efficiency decreased with the distance from the vacuum manifold, however, higher collection efficiencies were observed at plume locations 7-9 (Figure 14-15), although this was specific to plume velocities at 25 Ft/min and 6 Ft/min.

Effect of Plume Locations on PTS Collection Efficiency

Distance from the vacuum manifold was negatively associated with collection efficiency. Overall, plume locations on the row closest to the vacuum manifold (i.e., locations 1-3) had the highest collection efficiencies within the acceptable range (70-100%) at HVE flowrates of 100 Lpm and 200 Lpm (Figure 9-19). This is followed by the middle row (locations 4-6), followed by the row furthest from the manifold (locations 7-9). Due to the low collection efficiencies observed at plume locations 7-9 at HVE flowrate, plume locations 1 - 6 on the PTS should always be positioned at least 13 cm directly above the oral cavity during dental procedures as these locations tend to have higher collection efficiency. On the whole, the two best performing locations were the two center locations (locations 2 and 5), although this was not statistically significant different from the referent location (location 1).

Effects Plume Velocities on PTS Collection Efficiencies

Based on observation of the data output obtained from this study, plume velocity had minimal effect on the overall collection efficiency compared to HVE flowrates and plume locations. From As shown in Figure 9, plume location 3 (0%) and location 7-9 (0 - 14%), plume velocity of 50 Ft/min had the lowest collection efficiency at HVE flowrate of 100 Lpm compared to the other plume velocities. In addition, plume velocity of 50 Ft/min had the lowest (0%) collection efficiency at plume locations 7-9 (Figure 13). The highest collection efficiency was observed at plume velocity of 6 Ft/min at 100 and 200 Lpm, and 25 Ft/min at 200 Lpm (Figure 11 and 14).

PTS Collection Efficiency for Alveolic Particles

Figure 16-17 shows PTS collection efficiencies for alveolic particles at the various plume velocities and HVE flowrates. Higher PTS collection efficiencies for alveolic particles was observed at HVE flowrate of 200 Lpm. PTS Collection efficiency decreases with distance from the suction manifold. Plume locations 7-9 had the lowest collection efficiencies, especially at HVE flowrate of 100 Lpm. At HVE flowrate of 200 Lpm, plume location 9 had the lowest collection. These findings which are similar to those observed for particle count values (Figure 8-15) further shows how PTS is effective at capturing particles at HVE flowrate ≥200 Lpm.

While most of the literature reviewed focused on particle deposition in the respiratory tract, this study was much more practical in nature, seeking to identify the operation conditions most effective for dental aerosol collection and therefore most effective for the prevention of exposure to these aerosols, including pathogens. This study demonstrated that PTS has better collection efficiency at HVE flowrate of 200 Lpm compared to HVE flowrate of 100 Lpm. Although the plots of collection efficiency at various shield locations, plume velocities and HVE flow rates are useful for visualizing the effectiveness of the PTS, they are not capable of providing a statistical evaluation of the PTS performance. For statistical evaluation, mixed effect regression model was used. When constructing this model, each of the main effects and an interaction term between HVE flowrate and plume location were evaluated. As stated in the data analysis section of the methods section, HVE flow rate and plume location were modeled as fixed effects but plume velocity was modeled as a random effect due to the constantly changing nature of air currents within a dental clinic and the varied plume velocities generated by intermittent tool use. The interaction term, HVE flowrate versus Plume location was not significant and therefore was dropped for the final model. HVE flowrate had a significant effect on collection efficiency as expected. Plume location effect was significant for some locations but not all. Specifically, the effect of plume locations 7, 8, and 9 were significant for all particle sizes studied under all conditions (Figure 19-30). However, location 4 was significant only for particles 0.30 μm – 0.65 μm and 5.0 μm. Conversely, p-values for plume locations 2, 3 and 5 were not significant for 0.3 μm – 5.0 μm particle size bins. At first examination this may seem counter-intuitive, however this is due to the way the model was constructed. The model selected plume location 1 as the referent, which means the intercept term represents the effect and significance of location 1. All other plume locations are compared to location 1. Since the collection efficiency for the first row (locations 1-3) were similar and generally high, we should not expect a significant effect (difference) between location 1 and locations 2, 3, and 5.

Another way to interpret the model findings is as follows; locations 7-9 provided a consistent, significant negative effect on collection efficiency, locations 4 and 6 often have a significant, negatively effect on collection efficiency, but placement of the plume on locations 2, 3 and 5 does not have a significant

effect on collection efficiency compared to location 1. The practical implication of this is that clinicians should ensure effective capturing of particles ≤ 5 μm, by using the PTS at higher HVE flow rates and directing the plume to shield locations 1, 2, 3 or 5.

Figure 18 shows a summary of the data output obtained from the mixed effect linear regression model for particle count values. The P-values for plume locations 1-3 and 5 were not significant for particle size bins 0.3 um – 5 μm, meaning these locations were not significantly different from location 1. Alternatively, significant P-values were observed for plume locations 7,8,9 for particle size bins 0.3 μm – 5 μm, meaning that PTS collection efficiencies at these plume locations are significantly different from those at plume location 1. As shown in Figure 8-15, overall data shows plume locations 1-3 and 5 had the best collection efficiencies compare to the remaining locations and were not statistically significantly different from each other, but were significantly different from locations 7-9 all the time and locations 4 and 6 under some conditions. These data also agree with the overall R^2 values for particle size bin < 0.3 μm – 5 μm which shows approximately 70% of the variability in the collection efficiencies of PTS are attributed to the studied variables.

Based on these findings, spatial positioning, plume locations, plume velocities and HVE flowrates influenced PTS collection efficiency. To minimize exposure to dental aerosol, locations on the shield identified as 1,2,3 and 5 should be directly above the oral cavity or aerosol emission sources during dental procedures. These locations had the best collection efficiencies. In addition, HVE flowrate should be adjusted to at least 200 Lpm as these flowrates yielded high collection efficiency compared to 100 Lpm.

Limitations

There are many limitations of this work which leave room for future studies. A few of the key limitations are: 1) the particle sizes studied were ~5 μm and below. It is known that infectious material can be present in larger particles and some bacterium can be larger than this study's upper range of particles. Future studies should evaluate the capture efficiency of the PTS for inhalable particles from 5-100 μm. 2) the effect of particle droplet drying on the shield of PTS was not studied. In this study, the test aerosol was formed from dried NaCl solution that was generated by a nebulizer. In a dental clinic it is expected that

many larger particles will be formed and evaporate to smaller particles or possibly nuclei. The challenge aerosol were stable in these experiments. 3) the effect of shield distance from the oral cavity was not studied. We do not expect this to have any effect on the collection efficiency of the PTS, but as distance from the plume source increases the plume velocity is likely to decrease and the plume is expected to expand. Therefore, a study that assesses plume velocity and spread could be used with this fundamental characterization to predict PTS collection at different distances from the oral cavity and different operational conditions. 4) only a few values for HVE flow rate were characterized spanning the range of HVE flow rates observed in the OUCOD clinics. Further increasing HVE flow rate is expected to further improve the collection efficiency of the PTS and expand the 'reach' of the suction manifold, but this was not evaluated. 5) lastly, the effect of cross draft on the collection efficiency of PTS was observed in this study. At lower HVE flowrate and plume velocities, the natural, variable air current within the laboratory tended to drift particles off the plume centerline. This can be seen in the variability of the collection efficiency in location 3, especially at 6 and 25 Ft/min plume velocities. This effect is also expected to be present during the use of the PTS during clinical settings as evidenced by the widely ranging background velocities measured in Phase 1 of this study and the variability of dental aerosol plume velocity due to the intermittent use of dental instruments.

CHAPTER V

CONCLUSION

As expected, PTS collection efficiency increased with HVE flowrate. PTS was more effective in capturing 0.3 μm – 5 μm particles at HVE flowrate of 200 Lpm than at 100 Lpm and this is expected to scale with further increases in HVE flow rate and at flowrates between 100 and 200 Lpm. This study also found PTS collection efficiency was strongly influenced by plume locations. The overall collection efficiency of PTS at locations around the edges of the shield (i.e., locations 4, 6, and 7-9) significantly lower than the locations closest to the vacuum manifold. A visual indicator to remind PTS operators to place the dental plume at location 2 or 5 would help to prevent the misconception that all placements are equally effective. For example, at HVE flowrate of 200 Lpm, and plume velocities 6, 25, 50 and 100 Ft/min, the average collection efficiency for alveolic particles (Figure 17) at plume locations 2 and 5 are 99% and 84%. Plume locations 4 through 6 had an average collection efficiency of 75% and plume locations 7 through 9 had an average collection efficiency of 44% for alveolic particle at HVE flowrate of 200 Lpm. This demonstrates how PTS collection efficiencies decreases with increase in distance from the air suction manifold and closeness to the edge of the shield.

It must be emphasized that no single approach can eliminate the risk of infection to dental personnel or other patients. PTS is one of the first layers of defense against aerosol exposure that captures the contaminants at the source, and this study has provided evidence that support PTS as an engineering control tool with the potential to greatly reduce the risk of exposure to dental aerosol if properly utilized. The findings from this study are intended to guide dental personnel on how to use PTS, not establish a single "best" parameter for use. Dental personnel should ensure to constantly relocate the PTS so that it intercepts the dental aerosol plume with locations 2 and 5 of the PTS shield. Diligent utilization of the PTS is expected to greatly reduce fugitive dental aerosols and therefore greatly reduce the risk of dental aerosol exposure for the clinicians and patients.

LIST OF REFERENCES

Avasth, A. (2018). High Volume Evacuator (HVE) in reducing aerosol - an exploration worth by clinicians. *Journal of Dental Health Oral Disorders & Therapy***.** *9*(3). Retrieved from http://medcrave-online.com/JDHODT/JDHODT-09-00371.pdf

Baumann, K., Boyce, M., Martinez, D. (2018). Transmission precautions for dental aerosols. *Journal of Multidisciplinary Care.* Retrieved from https://decisionsindentistry.com/article/transmission-precautions-for-dental-aerosols/

Brown, J. S., Gordon, T., Price, O., & Asgharian, B. (2013). Thoracic and respirable particle definitions for human health risk assessment. *Particle and fibre toxicology*, *10*, 12. https://doi.org/10.1186/1743-8977-10-12

Blake, G. C. (1963). The Incidence and Control of Bacterial Infection in Dental Spray Reservoirs. *Brit. Dent. J.*, *115*(10), 413-16.

Center for Disease Control (2003). Guidelines for infection control in dental healthcare settings. Retrieved from https://www.cdc.gov/mmwr/preview/mmwrhtml/rr5217a1.htm

Chao, C., Wan, M. P., Morawska, L., Johnson, G. R., Ristovski, Z. D., Hargreaves, M., Mengersen, K., Corbett, S., Li, Y., Xie, X., & Katoshevski, D. (2009). Characterization of expiration air jets and droplet size distributions immediately at the mouth opening. *Journal of aerosol science*, *40*(2), 122–133. https://doi.org/10.1016/j.jaerosci.2008.10.003

Cai, C. and Floyd, E. L. (2020). Effects of Sterilization with Hydrogen Peroxide and Chlorine Dioxide on the Filtration Efficiency of N95, KN95, and Surgical Face Masks. *JAMA Network Open* **3**, e2012099, doi:10.1001/jamanetworkopen.2020.12099.

Chen, C., Zhao, B., Cui, W., Dong, L., An, N., & Ouyang, X. (2010). The effectiveness of an air cleaner in controlling droplet/aerosol particle dispersion emitted from a patient's mouth in the indoor environment of dental clinics. *Journal of the Royal Society, Interface*, *7*(48), 1105–1118. https://doi.org/10.1098/rsif.2009.0516

Chi-Yu, C., Hsin-Chung, C., Shinhao, Y., Wei, F., Po-Chen, H., Sheng-Yen, C (2014). Investigation of the spreading characteristics of bacterial aerosol contamination during dental scaling. *Journal of Dental Science, 9*(3)*, 294-296.* https://doi.org/10.1016/j.jds.2014.06.002

Environmental Protection Agency (2021). Particulate matter (PM) basics. Retrieved from https://www.epa.gov/pm-pollution/particulate-matter-pm-basics.

Dutil, S., Meriaux, A., de Latremoille, M. C., Lazure, L., Barbeau, J., & Duchaine, C. (2009). Measurement of airborne bacteria and endotoxin generated during dental cleaning. *Journal of occupational and environmental hygiene*, *6*(2), 121–130. https://doi.org/10.1080/15459620802633957

Esteban Florez, F. L., Thibodeau, T., Oni, T., Floyd, E., Khajotia, S. S., & Cai, C. (2021). Size-resolved spatial distribution analysis of aerosols with or without the utilization of a novel aerosol containment de-vice in dental settings. Physics of Fluids, 33(8), 085102.

Geisinger, M. (2020). Aerosols in the Dental Office: Best practices for patient and practitioner safety. Retrieved from https://www.dentalcare.com/en-us/professional-education/ce-courses/ce619/airborne-droplets

Gowtham, S., and Deepthi, P. (2014). Bioaerosol contamination in dental clinic: A potential health hazard? *Annals and Essence of Dentistry. doi: 10.5958/0976-156X.2014.00010.0*

Harrel, S. K., & Molinari, J. (2004). Aerosols and splatter in dentistry: a brief review of the literature and infection control implications. *Journal of the American Dental Association (1939)*, *135*(4), 429–437. https://doi.org/10.14219/jada.archive.2004.0207

Harrel S. K. (1996). Clinical use of an aerosol-reduction device with an ultrasonic scaler. *Compendium of continuing education in dentistry (Jamesburg, N.J.: 1995)*, *17*(12), 1185–1194.

Hinds, W. C. (1999). Aerosol technology: properties, behavior, and measurement of airborne particles. John Wiley & Sons.

Jacks M. E. (2002). A laboratory comparison of evacuation devices on aerosol reduction. *Journal of dental hygiene: JDH*, *76*(3), 202–206.

Jawade, R., Bhandari, V., Ugale, G., Taru, S., Khaparde, S., Kulkarni, A., Ardale, M., & Marde, S. (2016). Comparative Evaluation of Two Different Ultrasonic Liquid Coolants on Dental Aerosols. *Journal of clinical and diagnostic research: JCDR*, *10*(7), ZC53–ZC57. https://doi.org/10.7860/JCDR/2016/20017.8173

Jia, D., Lee Baker, J., Rameau, A., & Esmaily, M. (2021). Simulation of a vacuum helmet to contain pathogen-bearing droplets in dental and otolaryngologic outpatient interventions. *Physics of fluids (Woodbury, N.Y.: 1994)*, *33*(1), 013307. https://doi.org/10.1063/5.0036749

King, T. B., Muzzin, K. B., Berry, C. W., & Anders, L. M. (1997). The effectiveness of an aerosol reduction device for ultrasonic scalers. *Journal of periodontology*, *68*(1), 45–49. https://doi.org/10.1902/jop.1997.68.1.45

Koullapis, P. G., Kassinos, S. C., & Lin, C. L. (2015). Computational fluid dynamics (CFD) Simulations of aerosol deposition in the lungs. In *Ninth International Symposium on Turbulence and Shear Flow Phenomena*. Begel House Inc. Retrieved from Google Scholar.

Micik, R., Miller, R., Mazzarella, M., Ryge, G. (1969). Studies on dental aerobiology: Bacterial aerosols generated during dental procedures. *Journal of Dental Research 48*(1), 49-56.

Milejczak, C. (2005). Optimum Travel Distance of Dental Aerosols in the Dental Hygiene Practice. *Journal of Dental Hygiene.* 20-20. Retrieved from https://www.researchgate.net/publication/233718532_Optimum_Travel_Distance_of_Dental_Aerosols_in_the_Dental_Hygiene_Practice

Morawska L. (2006). Droplet fate in indoor environments, or can we prevent the spread of infection? *Indoor air*, *16*(5), 335–347. https://doi.org/10.1111/j.1600-0668.2006.00432.x

Murdoch-Kinch, C., Andrews, N., Atwan, S., Jude, R., Gleason, M., Molinari, J. (1997). Comparison of dental water quality management procedures. *Journal of American Dental Association*, *128*(9). DOI: https://doi.org/10.14219/jada.archive.1997.0400

National Institute for Occupational Safety and Health (1996). Guide to the Selection and Use of Particulate Respirators. Publication number 96-101. Retrieved from https://www.cdc.gov/niosh/docs/96-101/default.html

NIOSH (2019). Procedure no. TEB-APR-STP-0059. Retrieved from https://www.cdc.gov/niosh/npptl/stps/pdfs/TEB-APR-STP-0059-508.pdf

Nulty, A., Lefkaditis, C., Zachrisson, P., Van Tonder, Q., & Yar, R. (2020). A clinical study measuring dental aerosols with and without a high-volume extraction device. *British dental journal*, 1–8. Advance online publication. https://doi.org/10.1038/s41415-020-2274-3

Polednik, B. (2014). Aerosols and bioaerosols particles in dental office. *Environmental Research 134*, 405-409. https://doi.org/10.1016/j.envres.2014.06.027.

Putnins, E., Di Giovanni, D., & Bhullar, A. S. (2001). Dental unit waterline contamination and its possible implications during periodontal surgery. *Journal of periodontology*, *72*(3), 393–400. https://doi.org/10.1902/jop.2001.72.3.393

Sotiriou, M., Ferguson, S. F., Davey, M., Wolfson, J. M., Demokritou, P., Lawrence, J., Sax, S. N., & Koutrakis, P. (2008). Measurement of particle concentrations in a dental office. *Environmental monitoring and assessment*, *137*(1-3), 351–361. https://doi.org/10.1007/s10661-007-9770-7

Szymańska J. (2007). Dental bioaerosol as an occupational hazard in a dentist's workplace. *Annals of agricultural and environmental medicine: AAEM*, *14*(2), 203–207.

Shahdad S, Patel T, Hindocha A, Cagney N, Mueller JD, Seoudi N, et al. (2020). The efficacy of an extraoral scavenging device on reduction of splatter contamination during dental aerosol generating procedures: an exploratory study. Br Dent J. 2020 Sep 11 [Epub ahead of print]. Available from: https://doi.org/10.1038/s41415-020-2112-7

Taira, M., Sasaki, M., Kimura, S. and Araki, Y. (2009). Characterization of aerosols and fine particles produced in dentistry and their health risk assessments. *Nano Biomedicine 1*(1), 9-15. Retrieved from https://www.semanticscholar.org/paper/Characterization-of-Aerosols-and-Fine-Particles-in-Taira-Sasaki/cb51d1e6fb8338f1c32237887b15eb90575d4672

Tuttlebee, C. M., O'Donnell, M. J., Keane, C. T., Russell, R. J., Sullivan, D. J., Falkiner, F., & Coleman, D. C. (2002). Effective control of dental chair unit waterline biofilm and marked reduction of bacterial contamination of output water using two peroxide-based disinfectants. *Journal of Hospital Infection*, *52*(3), 192-205. doi:10.1053/jhin.2002.1282

Thomas, R. J., Webber, D., Sellors, W., Collinge, A., Frost, A., Stagg, A. J., Bailey, S. C., Jayasekera, P. N., Taylor, R. R., Eley, S., & Titball, R. W. (2008). Characterization and deposition of respirable large- and small-particle bioaerosols. *Applied and environmental microbiology*, *74*(20), 6437–6443. https://doi.org/10.1128/AEM.01194-08

Tang, Y., and Guo, B. (2011) Computational fluid dynamics simulation of aerosol transport and deposition. *Front. Environ. Sci. Eng. China* **5,** https://doi.org/10.1007/s11783-011-0365-8

Veena, H. R., Mahantesha, S., Joseph, P. A., Patil, S. R., & Patil, S. H. (2015). Dissemination of aerosol and splatter during ultrasonic scaling: a pilot study. *Journal of infection and public health*, *8*(3), 260–265. https://doi.org/10.1016/j.jiph.2014.11.004

Zemouri, C., Volgenant, C., Buijs, M., Crielaard, W., Rosema, N., Brandt, B., Laheij, De Soet, A. (2020) Dental aerosols: microbial composition and spatial distribution, *Journal of Oral Microbiology*, *12*(1), DOI: 10.1080/20002297.2020.1762040

APPENDIX A

			COLLECTION EFFICIENCY														
Flowrate	Plume velocity	Plume Location	0.3 um	0.4 um	0.50 um	0.65 um	0.3 um - 0.65 um Average	0.80 um	1.0 um	1.60 um	0.80 um - 1.60 um Average	2.00 um	3.00 um	4.00 um	5.00 um	2 um - 5 um Average	Alveolic [ug/m3]
100	100	l_1	0.7195548	0.7318	0.7412	0.84817	0.760	0.92103	0.9022	0.9486	0.924	0.9716	0.98416	0.93716	0.9449	0.96	0.922
100	100	l_2	0.9227077	0.9191	0.9207	0.9613	0.931	0.98145	0.9774	0.9874	0.982	0.994	0.99661	0.9831	0.9842	0.99	0.981
100	100	l_3	0.6997658	0.6658	0.6735	0.68737	0.682	0.69071	0.6746	0.6373	0.668	0.6741	0.68999	0.71886	0.8249	0.73	0.680
100	100	l_4	0.5881697	0.5612	0.5537	0.54604	0.562	0.51941	0.4861	0.403	0.469	0.4316	0.34683	0.32923	0.3529	0.37	0.510
100	100	l_5	0.8390731	0.8277	0.8368	0.8558	0.840	0.86244	0.8561	0.8372	0.852	0.8532	0.76915	0.66248	0.758	0.76	0.843
100	100	l_6	0.3994049	0.3585	0.3337	0.3109	0.351	0.26294	0.2205	0.1146	0.199	0.2475	0.09254	0.07445	0.2979	0.18	0.284
100	100	l_7	0.2636256	0.2001	0.147	0.04662	0.164	-0.0476	-0.1045	-0.2515	-0.135	-0.3116	-0.6916	-0.7821	-0.5651	-0.59	-0.037
100	100	l_8	0.0835701	0.0299	0.0286	-0.0037	0.035	-0.0695	-0.142	-0.3018	-0.171	-0.3258	-0.7898	-0.7485	-0.4096	-0.57	-0.106
100	100	l_9	-0.206049	-0.244	-0.2476	-0.5752	-0.318	-0.9305	-0.9458	-1.6038	-1.160	-1.7782	-2.4624	-1.9273	-1.3462	-1.88	-0.914
100	50	l_1	0.7845605	0.7893	0.7884	0.78527	0.787	0.7557	0.737	0.6397	0.711	0.7215	0.66757	0.68569	0.8081	0.72	0.755
100	50	l_2	0.9901628	0.99	0.9917	0.99482	0.992	0.99622	0.9956	0.9953	0.996	0.9957	0.98924	0.97227	0.9811	0.98	0.975
100	50	l_3	0.0679854	0.0067	-0.0428	-0.1061	-0.019	-0.1906	-0.2257	-0.2692	-0.229	-0.5586	-0.7325	-0.4876	-0.1176	-0.47	0.899
100	50	l_4	0.4698822	0.422	0.3625	0.27818	0.383	0.17559	0.0987	0.0269	0.100	-0.0687	-0.3039	-0.331	-0.2791	-0.25	0.195
100	50	l_5	0.104965	0.0946	0.1943	0.35637	0.188	0.43155	0.3872	0.3684	0.396	0.2672	0.00989	-0.0888	0.2381	0.11	0.525
100	50	l_6	0.4267959	0.347	0.3749	0.43552	0.396	0.47072	0.4356	0.3913	0.433	0.3705	0.11855	0.0365	0.1419	0.17	0.463
100	50	l_7	0.2412487	0.2296	0.1305	-0.2609	0.085	-0.7546	-0.8294	-1.5194	-1.034	-1.6789	-1.6125	-1.2088	-1.1067	-1.40	-0.135
100	50	l_8	0.2132832	0.1609	0.1243	0.0624	0.140	-0.0398	-0.103	-0.3439	-0.162	-0.2993	-0.43	-0.2838	-0.3239	-0.33	0.158
100	50	l_9	-0.248578	-0.236	-0.3873	-1.1807	-0.513	-2.1253	-2.244	-3.3374	-2.569	-4.3049	-4.3545	-3.227	-2.2336	-3.53	-0.635
100	25	l_1	0.7197873	0.7126	0.7356	0.78829	0.739	0.81431	0.8042	0.7667	0.795	0.773	0.72553	0.69388	0.5669	0.69	0.752
100	25	l_2	0.9651524	0.9636	0.9697	0.98179	0.970	0.9868	0.9839	0.9822	0.984	0.9794	0.96194	0.95249	0.937	0.96	0.993
100	25	l_3	0.8320468	0.8252	0.7612	0.8415	0.815	0.90341	0.8354	0.8872	0.875	0.9159	0.93231	0.89769	0.8415	0.90	-0.164
100	25	l_4	0.2991569	0.2064	0.1953	0.22012	0.230	0.21398	0.1465	0.0804	0.147	-0.0526	0.15475	0.23055	0.3716	0.18	0.213
100	25	l_5	0.3199982	0.2674	0.0983	0.35157	0.259	0.57212	0.3385	0.5326	0.481	0.5892	0.62452	0.28701	-0.0645	0.36	0.256
100	25	l_6	0.3276225	0.3083	0.0051	0.16773	0.202	0.52628	0.0243	0.4605	0.337	0.515	0.49064	0.28479	-0.0978	0.30	0.401
100	25	l_7	-0.023289	-0.038	-0.0411	-0.0587	-0.040	-0.0766	-0.1376	-0.0621	-0.092	-0.0982	-0.3645	-0.842	-1.0495	-0.59	-0.470
100	25	l_8	0.001215	-0.031	-0.2636	-0.0235	-0.079	0.21397	-0.0912	0.1909	0.105	0.2043	0.15277	-0.0659	-0.2532	0.01	-0.026
100	25	l_9	0.18911	0.1253	0.0031	-0.3917	-0.019	-0.8225	-0.9261	-1.3885	-1.046	-2.0108	-1.5544	-1.0276	-0.7255	-1.33	-1.663
100	6	l_1	0.8491755	0.8227	0.8165	0.83201	0.830	0.8345	0.816	0.7955	0.815	0.772	0.79683	0.75787	0.6609	0.75	0.825
100	6	l_2	0.654479	0.626	0.6276	0.68078	0.647	0.69842	0.6633	0.5818	0.648	0.6265	0.75362	0.74439	0.7635	0.72	0.649
100	6	l_3	0.424254	0.3693	0.3673	0.44425	0.401	0.47639	0.4167	0.3374	0.410	0.2777	0.30235	0.31319	0.3182	0.30	0.395
100	6	l_4	0.1175029	0.1545	-0.0171	0.09554	0.088	0.41818	0.0452	0.323	0.262	0.5157	0.66822	0.51768	0.5177	0.55	0.415
100	6	l_5	0.598733	0.5382	0.5309	0.55901	0.557	0.5643	0.5334	0.4432	0.514	0.5495	0.75341	0.66575	0.5532	0.63	0.559
100	6	l_6	0.443704	0.4384	0.2422	0.4431	0.392	0.73414	0.3692	0.6841	0.596	0.769	0.79305	0.69312	0.6874	0.74	0.703
100	6	l_7	0.1265231	0.1554	0.0743	0.2164	0.143	0.40558	0.1883	0.3148	0.303	0.4653	0.60752	0.29027	-0.028	0.33	0.369
100	6	l_8	0.2912143	0.2937	0.2275	0.33502	0.287	0.48297	0.329	0.4511	0.421	0.5363	0.68253	0.54255	0.5209	0.57	0.485
100	6	l_9	-0.132504	-0.111	-0.1004	-0.1522	-0.124	-0.0471	-0.2403	0.0313	-0.085	-0.0159	-1.0978	-1.0742	-1.0823	-0.82	-0.103
200	100	l_1	0.9653103	0.9698	0.9738	0.9899	0.975	0.99582	0.9945	0.9966	0.996	0.9984	0.99881	0.99541	0.9911	1.00	0.993
200	100	l_2	0.9961609	0.9966	0.997	0.99874	0.997	0.99944	0.9993	0.9995	0.999	0.9998	0.99971	0.99915	0.9955	1.00	0.999
200	100	l_3	0.9869555	0.9866	0.9893	0.99388	0.989	0.99584	0.9946	0.9942	0.995	0.9959	0.9942	0.99273	0.9869	0.99	0.992
200	100	l_4	0.7189768	0.7062	0.7229	0.76596	0.729	0.78075	0.7663	0.7174	0.755	0.771	0.64686	0.59143	0.6329	0.66	0.738
200	100	l_5	0.9836894	0.9836	0.9864	0.99185	0.986	0.99401	0.9925	0.9934	0.993	0.9912	0.95433	0.9214	0.9427	0.95	0.988
200	100	l_6	0.7892369	0.7959	0.7757	0.70277	0.766	0.61745	0.6065	0.4413	0.555	0.587	0.77164	0.81641	0.8638	0.76	0.672
200	100	l_7	0.0470044	0.0458	0.1746	0.44154	0.177	0.58599	0.5566	0.5373	0.560	0.6084	0.48327	0.33017	0.3841	0.45	0.374
200	100	l_8	0.2802644	0.256	0.3453	0.52052	0.351	0.61317	0.5859	0.5568	0.585	0.5875	0.41522	0.3278	0.2691	0.40	0.458
200	100	l_9	-0.492504	-0.598	-0.5148	-0.3934	-0.500	-0.3563	-0.4011	-0.4981	-0.418	-0.5744	-1.0783	-1.1454	-0.5	-0.82	-0.496
200	50	l_1	0.9890939	0.9871	0.9871	0.98988	0.988	0.99153	0.9908	0.989	0.990	0.9907	0.9876	0.97998	0.9535	0.98	0.906
200	50	l_2	0.9940916	0.9947	0.995	0.99626	0.995	0.99652	0.9964	0.9945	0.996	0.9965	0.98709	0.98614	0.9717	0.99	0.991
200	50	l_3	0.8744411	0.8852	0.9008	0.93315	0.898	0.94887	0.9463	0.9312	0.942	0.9567	0.95078	0.94837	0.9216	0.94	0.995
200	50	l_4	0.5662726	0.5526	0.5715	0.63466	0.581	0.65733	0.6303	0.5983	0.629	0.6176	0.26104	0.14318	-0.0543	0.24	0.399
200	50	l_5	0.5584778	0.5531	0.5966	0.66172	0.592	0.6864	0.6731	0.6025	0.654	0.726	0.8003	0.75087	0.7857	0.77	0.990
200	50	l_6	0.1959416	0.1319	0.2252	0.38921	0.236	0.47788	0.4553	0.3888	0.441	0.5788	0.59587	0.49664	0.3548	0.51	0.947
200	50	l_7	-0.283367	-0.344	-0.5069	-0.7987	-0.483	-1.1381	-1.2413	-1.5527	-1.311	-1.5441	-1.664	-1.6329	-1.6517	-1.62	0.816
200	50	l_8	-0.152204	-0.161	-0.132	-0.0226	-0.117	-0.0191	-0.0496	-0.1579	-0.076	-0.1284	-0.4143	-0.3372	-0.3521	-0.31	0.927
200	50	l_9	-1.636233	-1.61	-1.823	-2.452	-1.880	-3.2181	-3.4739	-4.1111	-3.601	-4.3898	-4.4724	-3.9151	-3.2991	-4.02	-0.280
200	25	l_1	0.8953784	0.8923	0.8987	0.92428	0.903	0.93783	0.9304	0.9255	0.931	0.9085	0.78056	0.7102	0.6433	0.76	0.989
200	25	l_2	0.9898398	0.9896	0.9905	0.99217	0.991	0.99345	0.9918	0.989	0.991	0.9922	0.98636	0.9819	0.9055	0.97	0.995
200	25	l_3	0.9488913	0.9555	0.9453	0.9869	0.959	0.9976	0.9928	0.9984	0.996	0.9989	0.99851	0.99152	0.9366	0.98	0.918
200	25	l_4	0.4499524	0.4255	0.418	0.44129	0.434	0.42494	0.3783	0.2867	0.363	0.306	0.29602	0.16234	-0.0541	0.18	0.587
200	25	l_5	0.9258175	0.9304	0.9237	0.97475	0.939	0.99276	0.9867	0.9956	0.992	0.9976	0.99714	0.98596	0.9513	0.98	0.635
200	25	l_6	0.4736372	0.5219	0.2116	0.74845	0.489	0.95432	0.831	0.9699	0.918	0.9857	0.98939	0.94604	0.8121	0.93	0.382
200	25	l_7	-0.212867	-0.105	-0.5727	0.23854	-0.163	0.82061	0.4478	0.8778	0.715	0.9363	0.9569	0.80333	0.0587	0.69	-0.848
200	25	l_8	0.3264642	0.395	0.1844	0.73957	0.411	0.93986	0.847	0.9606	0.916	0.9825	0.98702	0.93535	0.7434	0.91	-0.120
200	25	l_9	-0.156677	-0.302	-0.2945	-0.1932	-0.237	-0.1296	-0.1867	-0.309	-0.208	-0.2232	0.03549	-0.5592	-1.1961	-0.49	-2.749
200	6	l_1	0.9516562	0.9368	0.9302	0.93808	0.939	0.94381	0.9296	0.9185	0.931	0.9138	0.8859	0.88287	0.8908	0.89	0.936
200	6	l_2	0.9661953	0.9619	0.9639	0.97521	0.967	0.97814	0.9741	0.9616	0.971	0.9729	0.98213	0.97085	0.973	0.97	0.969
200	6	l_3	0.7122507	0.6855	0.6825	0.73993	0.705	0.7652	0.725	0.6464	0.712	0.6772	0.66239	0.62088	0.4242	0.60	0.703
200	6	l_4	0.7526237	0.7792	0.7466	0.89194	0.793	0.96961	0.9351	0.9828	0.963	0.9887	0.98716	0.90949	0.6839	0.89	0.964
200	6	l_5	0.7282642	0.7015	0.7206	0.81085	0.740	0.8482	0.8349	0.7979	0.827	0.7746	0.7076	0.55433	0.234	0.57	0.764
200	6	l_6	0.7584915	0.7814	0.7407	0.9074	0.797	0.98097	0.9478	0.9861	0.972	0.9942	0.99586	0.97569	0.9378	0.98	0.974
200	6	l_7	0.52122	0.6047	0.6444	0.85565	0.656	0.94811	0.9279	0.971	0.949	0.9839	0.97694	0.87714	0.646	0.87	0.927
200	6	l_8	0.06087	0.1613	0.1763	0.60118	0.250	0.85008	0.767	0.9082	0.842	0.9568	0.97451	0.86187	0.4561	0.81	0.840
200	6	l_9	0.2428915	0.3294	0.3557	0.64589	0.393	0.88134	0.7953	0.9444	0.874	0.9514	0.91939	0.67904	0.2152	0.69	0.850

Overall Average Collection Efficiencies by Flowrates, Plume Velocities, Plume Location, and Particle Size Bin (Reduced Data).

APPENDIX B

Below are representative raw data that were reduced and used to calculate collection efficiencies shown in Appendix A.

HVE (PTS) at 0 L/min and Plume velocity at 6 ft/min															
date & time	0.30 um	0.40 um	0.50 um	0.65 um	0.80 um	1.00 um	1.60 um	2.00 um	3.00 um	4.00 um	5.00 um	7.50 um	10.00 um	15.00 um	20.00 um
5/29/2021 3:38:13 PM	309680	171210	85670	21250	3650	3200	1350	820	60	20	0	0	0	0	0
5/29/2021 3:38:19 PM	4801640	3070200	1871260	674570	174140	135300	50080	13430	130	90	20	0	0	0	0
5/29/2021 3:38:25 PM	746620	441400	227110	48470	9020	8000	0	2580	1080	480	10	0	0	0	0
5/29/2021 3:38:31 PM	6538450	3687730	2557360	1121260	362970	293100	96150	45420	2780	1010	140	0	0	0	0
5/29/2021 3:38:37 PM	414700	254350	121890	26660	4910	3500	0	0	1570	780	100	0	0	0	0
5/29/2021 3:38:43 PM	5538550	3243380	1785450	597600	144810	115600	41730	13770	640	190	70	0	0	0	0
5/29/2021 3:38:49 PM	615220	390370	197800	42630	8620	7100	0	1650	1970	680	100	0	0	0	0
5/29/2021 3:38:55 PM	844270	593740	350580	83430	17130	14500	6660	2060	50	30	0	0	0	0	0
5/29/2021 3:39:01 PM	173730	103040	52530	12470	2750	2300	0	40	730	220	50	0	10	0	0
5/29/2021 3:39:07 PM	41890	25670	16680	4850	1050	1150	580	270	40	10	0	0	0	0	0
5/29/2021 3:40:20 PM	5133290	2695620	1346970	365340	80560	59450	21580	6710	520	130	10	0	0	0	0
5/29/2021 3:40:26 PM	372490	202210	100730	19090	4050	2550	0	1270	490	130	10	0	0	0	0
5/29/2021 3:40:32 PM	35760	22700	13020	4000	850	750	400	130	30	40	0	0	0	0	0
5/29/2021 3:40:38 PM	3537040	1643880	822850	204490	37900	29850	12010	3440	240	40	20	0	0	0	0
5/29/2021 3:40:44 PM	2072900	1065250	536580	122690	25490	17650	6140	3400	450	140	20	0	0	0	0
5/29/2021 3:40:50 PM	397400	217640	97010	21850	3900	3100	1400	220	50	20	10	0	0	0	0
5/29/2021 3:40:56 PM	3921170	1780060	851270	210710	42720	36150	13960	4010	120	40	20	0	0	0	0
5/29/2021 3:41:02 PM	1921880	939020	457650	101850	20000	15550	5200	2810	340	150	0	0	0	0	0
5/29/2021 3:41:08 PM	781590	447720	223380	48470	9020	7950	1500	1530	230	130	10	0	0	0	0
5/29/2021 3:41:14 PM	1876270	978000	487360	111670	20700	16200	6370	1850	20	10	0	0	0	0	0
5/29/2021 3:42:38 PM	785750	454170	226260	54330	11180	8100	3820	1860	120	80	20	0	0	0	0
5/29/2021 3:42:44 PM	377610	206570	111290	26620	5510	3800	2320	960	160	80	30	0	0	0	0
5/29/2021 3:42:50 PM	2218650	1130030	592840	140090	29670	22900	9640	3920	380	120	40	0	0	0	0
5/29/2021 3:42:56 PM	3830610	2075980	1141180	314740	70470	54750	13830	10180	1030	300	10	0	0	0	0
5/29/2021 3:43:02 PM	5449870	3076180	1581150	469190	104970	81100	25330	11230	810	400	30	0	0	0	0
5/29/2021 3:43:08 PM	1895570	1085490	587740	152800	31640	24400	10000	3200	250	160	40	0	0	0	0
5/29/2021 3:43:14 PM	1158530	583320	289820	66720	12540	11150	2870	2530	300	150	0	0	0	0	0
5/29/2021 3:43:20 PM	1946490	939050	468580	110760	21210	15600	6140	2790	330	150	40	0	0	0	0
5/29/2021 3:43:26 PM	4861980	2618240	1333440	377040	82240	65700	22840	9870	880	340	20	0	0	0	0
5/29/2021 3:43:32 PM	3933130	1938550	989870	265330	53140	42850	16330	5100	350	110	10	0	0	0	0
5/29/2021 3:45:01 PM	3472570	1975700	1112340	318100	68530	52200	20650	8410	780	300	60	0	0	0	0
5/29/2021 3:45:07 PM	6225270	3672530	2387590	892150	241120	187150	65310	20960	1030	280	70	0	0	0	0
5/29/2021 3:45:13 PM	6913090	3849870	2692280	1126040	342170	276150	100790	32090	1310	450	110	0	0	0	0
5/29/2021 3:45:19 PM	6028980	3563440	2272470	928160	278860	224450	67720	34390	2710	910	220	0	0	0	0
5/29/2021 3:45:25 PM	5988190	3628590	2211500	760490	190910	151400	48680	21060	1540	620	150	0	0	0	0
5/29/2021 3:45:31 PM	1582060	801940	396810	93980	18140	14550	6390	2600	240	150	20	0	0	0	0
5/29/2021 3:45:37 PM	1211470	666680	344000	77580	15510	13200	0	4860	1650	600	90	0	0	0	0
5/29/2021 3:45:43 PM	5492610	3063710	1617170	468830	109720	85450	32880	10140	510	170	90	10	0	0	0
5/29/2021 3:45:49 PM	5264080	2846940	1499800	456080	107500	80600	32540	10310	550	250	50	0	0	0	0
5/29/2021 3:45:55 PM	4393080	2241570	1227220	367170	82110	65900	23050	8250	700	200	50	0	0	0	0

Particle Count at Plume Location 1A-D (0 Lpm, 6 Ft/min)

HVE (PTS) at 100 L/min and Plume Velocity at 6 ft/min															
date & time	0.30 um	0.40 um	0.50 um	0.65 um	0.80 um	1.00 um	1.60 um	2.00 um	3.00 um	4.00 um	5.00 um	7.50 um	10.00 um	15.00 um	20.00 um
5/31/2021 8:51:52 AM	72850	45760	26110	7560	1400	1250	0	450	160	60	60	80	100	60	30
5/31/2021 8:51:58 AM	66080	43340	23500	6910	1700	1350	650	270	20	10	0	0	0	0	0
5/31/2021 8:52:04 AM	316480	254950	164700	40070	9620	7250	3750	1190	40	20	0	0	0	0	0
5/31/2021 8:52:10 AM	4202610	2924760	1920170	720970	209320	177000	71890	22390	420	160	40	0	0	0	0
5/31/2021 8:52:16 AM	79140	50180	28820	7210	2050	1600	0	0	470	300	70	10	0	0	0
5/31/2021 8:52:22 AM	71390	43520	25860	6810	1700	1500	810	200	50	40	0	0	0	0	0
5/31/2021 8:52:28 AM	3796710	2359130	1314240	400940	95280	83250	35380	10000	160	50	10	0	0	0	0
5/31/2021 8:52:34 AM	139760	91410	49050	11070	2450	2350	720	900	120	50	10	0	0	0	0
5/31/2021 8:52:40 AM	75340	49130	26910	7510	1450	1400	390	370	60	20	10	0	0	0	0
5/31/2021 8:52:46 AM	62810	39470	23600	6200	1200	1450	380	170	10	40	0	0	0	0	0
5/31/2021 8:54:20 AM	128160	82960	46430	11270	2250	2500	1160	450	30	10	0	0	0	0	0
5/31/2021 8:54:26 AM	137880	89790	48100	11320	2600	2650	250	750	190	60	0	0	0	0	0
5/31/2021 8:54:32 AM	162290	106310	57830	12070	3000	3000	0	1130	90	30	0	0	0	0	0
5/31/2021 8:54:38 AM	133420	78720	45130	10460	1950	2050	690	740	100	50	20	0	0	0	0
5/31/2021 8:54:44 AM	366990	233010	129910	26520	6010	5500	340	1910	280	90	30	0	0	0	0
5/31/2021 8:54:50 AM	266070	171510	95520	21840	4510	4200	1890	480	10	40	30	0	0	0	0
5/31/2021 8:54:56 AM	521750	345580	191000	41160	8120	7150	810	2960	320	220	30	10	0	0	0
5/31/2021 8:55:02 AM	1408350	816050	435730	102770	21850	20900	8750	2910	100	20	20	0	0	0	0
5/31/2021 8:55:08 AM	90700	56460	31840	8160	2000	1550	0	1190	80	120	10	0	0	0	0
5/31/2021 8:55:14 AM	613650	362590	200350	41180	8680	9250	970	3710	470	160	40	0	0	0	0
5/31/2021 8:56:35 AM	69330	45200	26410	7310	1250	1250	710	230	30	30	0	0	0	0	0
5/31/2021 8:56:41 AM	73770	48900	28220	7710	1600	1350	710	300	40	0	0	0	0	0	0
5/31/2021 8:56:47 AM	110420	69620	41640	8510	2200	1450	760	300	30	0	10	0	0	0	0
5/31/2021 8:56:53 AM	68030	42160	22450	6610	1900	1700	590	380	60	20	0	0	0	0	0
5/31/2021 8:56:59 AM	196920	125570	68550	16430	2950	2950	1210	820	60	30	30	0	0	0	0
5/31/2021 8:57:05 AM	79350	50530	28120	7410	1500	1400	660	860	100	30	0	0	0	0	0
5/31/2021 8:57:11 AM	85480	57150	28370	8310	1550	1150	490	180	30	0	0	0	0	0	0
5/31/2021 8:57:17 AM	68890	42040	24810	7260	1450	2150	610	310	10	20	0	0	0	0	0
5/31/2021 8:57:23 AM	185800	123070	65820	15480	3100	3000	1650	610	10	30	0	0	0	0	0
5/31/2021 8:57:29 AM	332780	208210	109410	25270	5060	5200	2770	830	50	0	0	0	0	0	0
5/31/2021 8:58:45 AM	245060	156830	79370	17740	3800	3550	0	1150	510	240	40	0	10	0	0
5/31/2021 8:58:51 AM	435160	270060	144460	32810	6770	6850	1880	2410	260	90	10	0	0	0	0
5/31/2021 8:58:57 AM	85490	56230	30740	8160	1850	2000	810	200	60	30	0	0	0	0	0
5/31/2021 8:59:03 AM	158010	96770	54270	13920	3050	3500	1230	380	40	30	20	0	0	0	0
5/31/2021 8:59:09 AM	195560	131570	67180	14880	3600	3500	1330	690	50	20	10	0	0	0	0
5/31/2021 8:59:15 AM	81470	49360	29530	8860	1600	1750	1180	380	80	40	20	0	0	0	0
5/31/2021 8:59:21 AM	72830	47640	27420	9310	1500	1500	650	260	20	20	0	0	0	0	0
5/31/2021 8:59:27 AM	104210	64680	37540	10210	2500	2650	730	490	80	30	20	0	0	0	0
5/31/2021 8:59:33 AM	1320340	890070	548820	145200	30920	25850	9980	6390	680	200	50	0	0	0	0
5/31/2021 8:59:39 AM	377540	239300	126710	26530	6610	4950	1990	1370	140	50	0	0	0	0	0

Particle counts at Plume Location 1A-D (100 Lpm, 6 Ft/min)

HVE (PTS) at 200 L/min and Plume Velocity at 6 Ft/min															
date & time	0.30 um	0.40 um	0.50 um	0.65 um	0.80 um	1.00 um	1.60 um	2.00 um	3.00 um	4.00 um	5.00 um	7.50 um	10.00 um	15.00 um	20.00 um
5/31/2021 4:45:46 PM	10240	6510	3750	350	200	100	0	90	60	40	10	0	0	0	0
5/31/2021 4:45:52 PM	190960	343490	305410	98700	23670	22450	9470	2780	0	0	0	0	0	0	0
5/31/2021 4:45:58 PM	825630	546820	318820	79690	15180	15200	7720	2870	200	60	0	0	0	0	0
5/31/2021 4:46:04 PM	10690	5660	3350	650	50	400	0	50	0	0	0	0	0	0	0
5/31/2021 4:46:10 PM	8670	5210	2700	650	50	100	40	10	0	0	0	0	0	0	0
5/31/2021 4:46:16 PM	37540	26280	14120	2900	400	650	0	40	280	60	20	0	0	0	0
5/31/2021 4:46:22 PM	8120	6260	2900	800	50	150	0	0	0	0	0	0	0	0	0
5/31/2021 4:46:28 PM	43410	29780	15220	3450	900	850	0	280	70	40	10	0	0	0	0
5/31/2021 4:46:34 PM	1826330	1361400	920280	314760	76520	80100	30180	13940	1080	410	90	0	0	0	0
5/31/2021 4:46:40 PM	935420	568610	320680	75030	16480	13600	6340	3220	540	210	40	0	0	0	0
5/31/2021 4:48:02 PM	22280	14810	8910	2350	200	450	130	50	10	10	0	0	0	0	0
5/31/2021 4:48:08 PM	7520	5560	1800	750	100	200	0	40	0	10	0	0	0	0	0
5/31/2021 4:48:14 PM	8570	5010	2900	600	150	150	80	20	0	0	0	0	0	0	0
5/31/2021 4:48:20 PM	6360	3960	3000	850	200	100	140	10	0	0	0	0	0	0	0
5/31/2021 4:48:26 PM	7770	5160	3000	800	100	200	0	0	0	0	0	0	0	0	0
5/31/2021 4:48:32 PM	7920	4660	2350	1300	200	200	90	10	0	0	0	0	0	0	0
5/31/2021 4:48:38 PM	7220	5460	2450	850	50	150	0	0	0	0	0	0	0	0	0
5/31/2021 4:48:44 PM	6310	4910	2400	450	50	100	120	30	0	0	0	0	0	0	0
5/31/2021 4:48:50 PM	7460	4610	2350	650	200	100	20	20	0	10	0	0	0	0	0
5/31/2021 4:48:56 PM	8770	4860	2450	800	150	50	0	0	0	0	0	0	0	0	0
5/31/2021 4:49:57 PM	11530	7310	5500	1100	300	100	120	60	20	0	0	0	0	0	0
5/31/2021 4:50:03 PM	14630	8410	4600	800	300	200	40	140	20	0	0	0	0	0	0
5/31/2021 4:50:09 PM	570240	366940	204210	42500	10310	8000	4570	1410	80	40	0	0	0	0	0
5/31/2021 4:50:15 PM	14440	9510	4400	700	500	600	20	80	0	0	0	0	0	0	0
5/31/2021 4:50:21 PM	14540	8310	4500	800	300	500	220	120	60	0	0	0	0	0	0
5/31/2021 4:50:27 PM	13330	9210	5100	1100	200	100	0	0	0	0	0	0	0	0	0
5/31/2021 4:50:33 PM	23290	16840	8100	1600	0	500	280	0	20	0	0	0	0	0	0
5/31/2021 4:50:39 PM	11430	9010	4300	800	100	100	200	100	0	0	0	0	0	0	0
5/31/2021 4:50:45 PM	30680	26780	10700	2000	700	200	0	180	60	40	20	0	0	0	0
5/31/2021 4:50:51 PM	446090	297050	160500	38670	7510	8400	2690	590	20	0	0	0	0	0	0
5/31/2021 4:51:54 PM	49130	34160	18010	3600	800	1100	340	100	40	20	0	0	0	0	0
5/31/2021 4:52:00 PM	19060	11120	6700	1200	400	300	120	80	0	0	0	0	0	0	0
5/31/2021 4:52:06 PM	13030	7710	4200	1300	400	600	160	60	80	0	0	0	0	0	0
5/31/2021 4:52:12 PM	168690	117980	59030	10810	2600	1600	0	0	400	200	0	0	0	0	0
5/31/2021 4:52:18 PM	14840	9010	4200	1200	300	200	0	0	0	0	0	0	0	0	0
5/31/2021 4:52:24 PM	13430	9410	3200	1800	100	100	10	30	40	20	0	0	0	0	0
5/31/2021 4:52:30 PM	11930	8910	5200	1800	300	100	140	60	0	0	0	0	0	0	0
5/31/2021 4:52:36 PM	12930	8910	4300	800	100	200	0	80	20	0	0	0	0	0	0
5/31/2021 4:52:42 PM	14730	7310	5400	300	0	300	0	180	0	20	0	0	0	0	0
5/31/2021 4:52:48 PM	12720	7210	3600	1000	100	100	0	0	0	0	0	0	0	0	0

Particle Count for Plume Location 1A-D at 200 Lpm and 6 Ft/min

HVE (PTS) at 0 L/min and Plume velocity at 6 ft/min						
date & time	PM10 [ug/m3]	PM2.5 [ug/m3]	PM1 [ug/m3]	Inhalable [ug/m3]	Thoracic [ug/m3]	Alveolic [ug/m3]
5/29/2021 3:38:13 PM	148.5	135.7	102.2	151	150.9	144.5
5/29/2021 3:38:19 PM	3152.3	3007.3	2000.3	3208.4	3207.8	3121.5
5/29/2021 3:38:25 PM	451.4	318.6	247.5	467	466.1	400.4
5/29/2021 3:38:31 PM	5865.5	5160.3	3033	6029.8	6025.4	5717.9
5/29/2021 3:38:37 PM	353.4	162.4	134.1	376.4	373.2	262.9
5/29/2021 3:38:43 PM	3169.5	2971.2	2076.7	3226.8	3225	3108.2
5/29/2021 3:38:49 PM	484.2	269.3	207.6	510.2	507.1	391.1
5/29/2021 3:38:55 PM	481.7	456.7	324	489.3	489.2	473.8
5/29/2021 3:39:01 PM	157.8	72.9	58.3	183	166.5	112.8
5/29/2021 3:39:07 PM	33.7	28.1	17.1	34.7	34.7	32.4
5/29/2021 3:40:20 PM	2302	2197.6	1700.2	2330.8	2330.3	2259.2
5/29/2021 3:40:26 PM	201.2	148.1	117.7	207.5	207.1	181.6
5/29/2021 3:40:32 PM	28.2	21.1	13.8	29.3	29.2	25.4
5/29/2021 3:40:38 PM	1439.4	1385.9	1116.8	1454.9	1454.4	1413.1
5/29/2021 3:40:44 PM	911.7	837.1	664.9	925.5	924.9	881
5/29/2021 3:40:50 PM	162.3	152.8	124	164.5	164.3	156.1
5/29/2021 3:40:56 PM	1583.1	1530.4	1225	1600.3	1599.8	1557.6
5/29/2021 3:41:02 PM	807.1	747.7	601.8	817.9	817.7	783.2
5/29/2021 3:41:08 PM	363.8	321.3	254.9	370.5	370.1	345.6
5/29/2021 3:41:14 PM	766.6	747.4	600.2	773.6	773.6	755.7
5/29/2021 3:42:38 PM	386.3	348.7	262.2	393.9	393.4	370.7
5/29/2021 3:42:44 PM	207.4	173.4	127.6	213.5	212.7	191.9
5/29/2021 3:42:50 PM	1024.4	945	727.3	1041.5	1040.5	991.8
5/29/2021 3:42:56 PM	1957.6	1777.5	1330.7	1991.5	1990.8	1900.5
5/29/2021 3:43:02 PM	2740.2	2544.8	1895.5	2784.6	2783.4	2669
5/29/2021 3:43:08 PM	945	874.4	657.2	961.4	960.4	913.3
5/29/2021 3:43:14 PM	524.3	469.6	369.4	533.2	533	504.5
5/29/2021 3:43:20 PM	839	769.3	615.3	852.6	851.5	806.9
5/29/2021 3:43:26 PM	2378.9	2201.4	1649.4	2417.7	2416.8	2316.6
5/29/2021 3:43:32 PM	1730	1650.8	1285.7	1751.6	1751.3	1698
5/29/2021 3:45:01 PM	1875.5	1709.4	1244	1911.4	1909.7	1815.1
5/29/2021 3:45:07 PM	4287.4	3994.3	2620.3	4374.6	4372.7	4219.2
5/29/2021 3:45:13 PM	5538.1	5098.5	3113.3	5670	5667	5456.6
5/29/2021 3:45:19 PM	4864.8	4254.7	2635	4998.8	4992.8	4701.2
5/29/2021 3:45:25 PM	3930.2	3551.4	2401.1	4017.9	4013.9	3810.3
5/29/2021 3:45:31 PM	708.3	650.2	506.8	720.1	719.4	683.6
5/29/2021 3:45:37 PM	736	518.9	398.4	763.8	761.1	649
5/29/2021 3:45:43 PM	2792.6	2624.5	1925.7	2841.6	2837.3	2723.4
5/29/2021 3:45:49 PM	2684.4	2520.5	1841.7	2728.6	2727.2	2626.4
5/29/2021 3:45:55 PM	2195.5	2049.3	1522.5	2231.6	2230.2	2143.1

PM Values for Plume Location 1A-D.

HVE (PTS) at 200 L/min and Plume Velocity at 6 Ft/min							
date & time	PM10 [ug/m3]	PM2.5 [ug/m3]	PM1 [ug/m3]	Inhalable [ug/m3]	Thoracic [ug/m3]	Alveolic [ug/m3]	
5/31/2021 4:45:46 PM	16.2	5.2	3.5	17.7	17.4	10.8	
5/31/2021 4:45:52 PM	400.2	374.4	200.4	410.2	410.2	398.9	
5/31/2021 4:45:58 PM	502.8	459.3	312.7	512.9	512.8	491.4	
5/31/2021 4:46:04 PM	5.8	5.4	3.8	6	6	5.8	
5/31/2021 4:46:10 PM	3.8	3.7	2.9	3.9	3.9	3.8	
5/31/2021 4:46:16 PM	44	17.7	13.3	47.3	46.8	32.1	
5/31/2021 4:46:22 PM	3.5	3.5	2.9	3.5	3.5	3.4	
5/31/2021 4:46:28 PM	35.5	22.3	15.7	37.3	37.1	29.6	
5/31/2021 4:46:34 PM	1757.8	1505.5	876.8	1812.4	1809.9	1689.8	
5/31/2021 4:46:40 PM	565.1	474.1	334.5	580.7	579.6	530.7	
5/31/2021 4:48:02 PM	13.7	11.6	8.4	14	14	12.9	
5/31/2021 4:48:08 PM	5.2	3.7	2.6	5.4	5.3	4.5	
5/31/2021 4:48:14 PM	4.6	4.4	3.1	4.7	4.7	4.6	
5/31/2021 4:48:20 PM	4.4	4.3	2.7	4.5	4.5	4.4	
5/31/2021 4:48:26 PM	3.6	3.6	2.9	3.6	3.6	3.6	
5/31/2021 4:48:32 PM	4.7	4.6	3.1	4.8	4.8	4.7	
5/31/2021 4:48:38 PM	3.2	3.2	2.6	3.2	3.2	3.1	
5/31/2021 4:48:44 PM	4.1	3.8	2.3	4.2	4.2	4.1	
5/31/2021 4:48:50 PM	4.8	3.5	2.6	5	4.9	4.2	
5/31/2021 4:48:56 PM	3.3	3.3	2.9	3.3	3.3	3.3	
5/31/2021 4:49:57 PM	8.4	6.8	4.6	8.6	8.6	8	
5/31/2021 4:50:03 PM	10	7.7	5	10.3	10.3	9.5	
5/31/2021 4:50:09 PM	308.8	287.1	204.3	314.2	314.1	301.9	
5/31/2021 4:50:15 PM	8.7	8	5.3	8.9	8.9	8.6	
5/31/2021 4:50:21 PM	13.9	9.8	5.4	14.5	14.5	13	
5/31/2021 4:50:27 PM	5.4	5.4	4.7	5.4	5.4	5.3	
5/31/2021 4:50:33 PM	12.8	11.8	8.2	13.1	13.1	12.5	
5/31/2021 4:50:39 PM	8	7.1	4.1	8.3	8.3	7.9	
5/31/2021 4:50:45 PM	28.9	14.4	10.6	31.1	30.6	21	
5/31/2021 4:50:51 PM	227.4	221.1	162.4	230.3	230.3	224.7	
5/31/2021 4:51:54 PM	30.6	25.5	17.9	31.4	31.4	28.6	
5/31/2021 4:52:00 PM	10.4	9.7	6.8	10.6	10.6	10.3	
5/31/2021 4:52:06 PM	13.6	9.1	5.2	14.1	14.1	12.4	
5/31/2021 4:52:12 PM	110.3	68.4	57	114.7	114.4	92	
5/31/2021 4:52:18 PM	5.9	6	5	6	6	5.9	
5/31/2021 4:52:24 PM	10.3	5.8	4.5	10.7	10.7	8.4	
5/31/2021 4:52:30 PM	7.8	7.3	4.9	8	8	7.7	
5/31/2021 4:52:36 PM	7.8	6.1	4.4	8	8	7.4	
5/31/2021 4:52:42 PM	11.6	7.7	5	12.1	12.1	10.3	
5/31/2021 4:52:48 PM	4.7	4.7	4.1	4.7	4.7	4.6	

PM Values at 200 Lpm and 6 Ft/min

APPENDIX C

Prototype Pro-TecT Shield

Experimental Setup

ProQuest Number: 28775044

INFORMATION TO ALL USERS
The quality and completeness of this reproduction is dependent on the quality
and completeness of the copy made available to ProQuest.

Distributed by ProQuest LLC (2022).
Copyright of the Dissertation is held by the Author unless otherwise noted.

This work may be used in accordance with the terms of the Creative Commons license
or other rights statement, as indicated in the copyright statement or in the metadata
associated with this work. Unless otherwise specified in the copyright statement
or the metadata, all rights are reserved by the copyright holder.

This work is protected against unauthorized copying under Title 17,
United States Code and other applicable copyright laws.

Microform Edition where available © ProQuest LLC. No reproduction or digitization
of the Microform Edition is authorized without permission of ProQuest LLC.

ProQuest LLC
789 East Eisenhower Parkway
P.O. Box 1346
Ann Arbor, MI 48106 - 1346 USA